D0 note 2066
August 23, 1995

The MTC Package
(Muon Tracking in the D0 Calorimeter)

Elizabeth Gallas

University of Texas at Arlington

Contents

List of Tables

List of Figures

1 Introduction

The MTC (Muon Tracking in the Calorimeter) package uses calorimeter information to identify and reconstruct track-like energy deposition in the calorimeter. This note describes how to use the MTC package and provides a brief description of the algorithms used in the package.

Though the calorimeter's transverse segmentation is coarse (in comparison to the D0 muon chambers) calorimeter track identification is possible because

- penetrating particles are fairly well isolated in the hadronic section of the calorimeter,
- the calorimeter longitudinal segmentation is sufficient to sample the energy deposited layer by layer, making isolated μ identification possible,
- the calorimeter hermeticity insures a uniform tracking efficiency as a function of η (pseudorapidity) and ϕ with no gaps in coverage,
- because there is no central magnetic field, muon tracks traverse a straight path in the calorimeter,
- muons generally emerge from a known vertex point (measured in the central tracking chambers) which provides a useful constraint to the calorimeter muon tracking, and
- muons typically deposit minimum ionizing energy over many radiation lengths, leaving a distinctive energy signature over the total path length.

The MTC package exploits these features to identify and track muons through the calorimeter.

The MTC package contains two utilities:

- The MTC μ identification utility performs muon identification and tracking of candidate tracks through the calorimeter.
- The MTC μ finding program provides an independent means for locating muon candidates.

D0 note 2068 describes some of the initial testing of the MTC μ identification utility performed before the package was in test release. The MTC μ identification utility has been incorporated into D0RECO event reconstruction. If your data set was RECO'd with V12.11 or higher, all MTC μ id information is stored in Zebra bank MTCA, and selected MTC id words are stored in the PMUO bank (see D0ZEBROOT:[MUDAT]PMUO.ZEB) for all muons in the MUON bank.

2 MTC Overview

The MTC package currently contains 2 utilities:

1. **MTC μ identification utility**

   Given a vertex position and an input direction (eta, phi) of a candidate muon (ie from PMUO), this utility looks at the energy deposition in the calorimeter cells in a road surrounding the μ candidate. Output information from this utility includes

   - track verification information
   - a reconstructed calorimeter track segment for isolated and non-isolat track-like objects in that calorimeter road,
   - track and road energy χ^2s, which indicate the level of muon isolation in the road,
   - a calorimetric measure of punchthrough, and
   - a calorimeter layer number at which muons seem to emerge from a more energetic object (a jet).

   This information can be used for

   - fake muon rejection,
   - ruling out the presence of a muon in a given direction,
   - vertex verification, and
   - global fitting of muon tracks in the D0 detector.

2. **MTC μ finding utility**

   Given an event vertex position, this utility scans the calorimeter for candidate tracks emerging from the vertex, providing an independent method for muon finding to

   - improve muon finding efficiency over all regions of the detector, and
   - provide an independent method for calculating muon system efficiencies.

3 Instructions for Use

Because calorimeter cell energies are required, input datasets must contain CAEP or CAEQ banks (available in Run1a STA's or Run1b STA and DST's). See D0$PBD:MTC.PBD to add MTC to your combined package, which must include CALOR and CAHITS to fill the necessary calorimeter cell energy banks. The D0$PBD:MTC.PBD file specifies the required object libraries, hooks, and necessary RCP files for both MTC utilities.

For example, the following program builder command

```
$ PBD/FRAME=D0USER -
  /PACKAGES=(CALOR,CAHITS,MTC)/NAME=DST -
  /ZEBCOM=5000000/PAWC=2000000 -
  /ZEBSTP=500000/ZEBWRK=160000 -
  /GCBANK=20000 -
  /LOG
```

will build a package with all the necessary features for running any of the MTC utilities.

3.1 MTC μ Identification Utility

A call to this utility is currently included starting with RECO V12.11 for all muon candidates in the MUON bank. If you are looking at Run Ib data, the MTC information may already be available.

- All MTC output information (described below) is stored in the event Zebra tree in bank MTCA hanging off each MUON bank.
- In addition, eleven of the most useful pattern recognition and muon verification words are stored in the PMUO bank (see the PMUO bank description in D0ZEBROOT:[MUDAT]PMUO.ZEB).

For RECO V12.11− processed data, in addition to storing the MTC output, MTC information is also used for vertex verification in some muon final state analyses.

If the MTC μ identification utility has not yet been run for your muon candidate track, then start by building your program using the MTC program builder package as described above. For each muon candidate for which you would like calorimeter μ identification information:

CALL MTC_MUCALTRACK(VTX(3), DVTX(3), ETA, PHI)

where	VTX(3)	= vertex (x, y, z) coordinates in cm
	DVTX(3)	= uncertainty in vertex coordinates
	ETA	= η of candidate track
	PHI	= ϕ of candidate track

The input vertex must be located inside the central detector volume.

A call to this routine fills the common block MTC as declared in the file D0$INC:MTC.INC :

```
COMMON /MTC/
        IMTC_MAX, IMTC_HMAX, IMTC_GHMAX, IMTC_LYRMU,
        XMTC_DIRCOS(3), XMTC_POINT(3), XMTC_TRES,
        XMTC_FRACT, XMTC_HFRACT, XMTC_GHFRACT, XMTC_ECHI,
        XMTC_DIRCOS_V(3), XMTC_POINT_V(3), XMTC_TRES_V,
        XMTC_EN5, XMTC_EN3, XMTC_EFRACT_H(1:3),
        XMTC_ECHI_33, XMTC_FRACT_33,
        XMTC_ECHI_55, XMTC_FRACT_55,
        XMTC_FRACH_33, XMTC_FRACH_55,
        XMTC_ECHI2
```

The above words contain tracking, energy χ^2, punchthrough and pattern recognition informat[illegible] as described in the subsections below. The tracking method and the χ^2 calculation are described in detail in a later section.

TRACK FIT RESULTS

Given the input vertex position and the η and ϕ of the track candidate, the program first locates the calorimeter cells along that candidate's trajectory in each layer. I call this set of cells the **'central tower'**. The program then defines a road in the calorimeter which extends .2 in η and .2 in ϕ from the central tower in each layer. This road is called the '5×5 **tower**' because it contains a 5×5 square array of cells in each layer (a total of 25 calorimeter cells in each layer). An analogous '3×3 **tower**' is also referred to below, containing 9 cells per layer centered on the central tower.

I define a *'hit'* cell as any calorimeter cell with a positive energy above zero suppression. The best calorimeter muon track is found by fitting a line through the longest set of contiguously hit calorimeter cells projected from the hadronic section toward the vertex in the 5×5 tower. The best calorimeter muon track segment as specified in the following variables includes the vertex posi[illegible] in the fit.

XMTC_DIRCOS_V(3) - the direction cosines of the best fit line

XMTC_POINT_V(3) - an arbitrary point on the best fit line (the direction cosines and one point uniquely defines the fit line)

XMTC_TRES_V - The track residual is the square root of the sum of the squares of the residuals of the fit points to the 3-D fit line divided by the number of points used in the fit. A reasonable track should have a track residual less than 10.

The calorimeter muon track segment specified in the variables below **does not** include the vertex in the fit.

XMTC_DIRCOS(3) - the direction cosines of the best fit line

XMTC_POINT(3) - a point on the best fit line

XMTC_TRES - track residual for this track fit

TRACK CONTINUITY

For the track fits described above, the following variables correspond to the fraction of calorimeter layers used as well as the maximum number of layers traversed by the track. Calorimeter muon track quality depends on the fraction of calorimeter layers used to get a fit; Ideally, good muons will have XMTC_FRACT = 1., meaning all possible layers were utilized for the track fit. I suggest that your good muon criteria include the following: require at least XMTC_FRACT $\geq$ 0.50 and XMTC_HFRACT $\geq$ 0.60.

IMTC_MAX - total number of layers available in the calorimeter along the direction of the calorimeter track

XMTC_FRACT - fraction of calorimeter layers used for the track fit out of the maximum possible (IMTC_MAX)

IMTC_HMAX - number of hadronic layers available in the calorimeter along the direction of the calorimeter track (a subset of IMTC_MAX)

XMTC_HFRACT - fraction of hadronic calorimeter layers used for the track fit out of the maximum possible (IMTC_HMAX)

IMTC_GHMAX - number of massless gap/icd/hadronic layers available in the calorimeter along the direction of the calorimeter track (a subset of IMTC_MAX)

XMTC_GHFRACT - fraction of massless gap/icd/hadronic calorimeter layers used for the track fit out of the maximum possible (IMTC_GHMAX)

MUON ISOLATION

The energy χ^2 is defined fully in a later section. In short, an isolated muon in the calorimeter will be characterized by a high fraction of layers hit (at least XMTC_FRACT $\geq$ 0.50 and XMTC_HFRACT $\geq$ 0.60.) and a low $\chi^2(\chi^2 \leq 5.0)$. A number of χ^2's can be calculated for a given track depending on the size of the calorimeter road used about that track, as shown below.

XMTC_ECHI - track χ^2 - a measure of the μ-likeness of the calorimeter track. This χ^2 is calculated based only on the energies of the cells used to get the track fit.

XMTC_ECHI_33 - '3×3 tower χ^2' - the χ^2 formed using the total energy deposited within the '3×3' array of adjacent cells in each layer. Isolated muons will have a low 3×3 tower $\chi^2(< 2.5)$ and a high fraction of layers hit (XMTC_FRACT_33= 1.).

XMTC_FRACT_33 - fraction of layers hit in the 3×3 tower.

XMTC_FRACH_33 - fraction of hadronic layers hit in the 3×3 tower.

XMTC_ECHI_55 - '5×5 tower χ^2' - the χ^2 formed using the total energy deposited within the '5×5' array of adjacent cells in each layer. Really isolated muons will have a low 5×5 tower $\chi^2(< 2.5)$ and a high fraction of layers hit (XMTC_FRACT_55= 1.).

XMTC_FRACT_55 - fraction of layers hit in the 5×5 tower.

XMTC_FRACH_55 - fraction of hadronic layers hit in the 5×5 tower.

TRACK AND TOWER ENERGY, PUNCHTHROUGH INFORMATION

XMTC_ETRACK - the calorimeter energy associated with the best track found. It is literally the sum of the energy of the hit calorimeter cells used to get the best calorimeter track fit.

XMTC_EN3 - the total calorimeter energy found in the 3×3 calorimeter tower.

XMTC_EN5 - the total calorimeter energy found in the 5×5 calorimeter tower.

XMTC_EFRACT_H(1:3) - fraction of the total 3×3 calorimeter energy found in the last, last two, and last 3 layers of the calorimeter, ie
XMTC_EFRACT_H(1) - fraction of energy in last layer
XMTC_EFRACT_H(2) - fraction of energy in last 2 layers
XMTC_EFRACT_H(3) - fraction of energy in last 3 layers

PATTERN RECOGNITION

It is possible to determine when a muon emerges from a more energetic object (a 'jet') by looking at the terms in the energy χ^2 layer by layer. The track is said to emerge from the jet when the measured average χ^2 of the track beyond that layer is ≤ 5.0.

IMTC_LYRMU - layer number at which the muon appears to emerge from a region of higher energy deposition (the 'jet'). This layer number is zero (0) if ALL calorimeter cells used in the fit had an average μ-like energy signature. It is 18 (calorimeter layer numbers range from 1 to 17) if the last layer utilized had an energy a bit more than one would expect for a μ-like particle.

XMTC_ECHI2 - an energy chi square of the track summed over all layers after the muon emerges from the 'jet'.

3.2 MTC μ Finding Utility

To use the MTC μ finding utility, start by building your program as in the beginning of this section. A number of user defined input parameters are available in MTC.RCP. Their default values are:

FULL_MTC	=	*.FALSE.*
MTC_ETAMIN	=	**0.0**
MTC_ETAMAX	=	5.0
MTC_HFRACSCAN	=	0.57
MTC_HFRACFND	=	0.60
MTC_FRACFND	=	0.50
MTC_IPSTATUS	=	1

To enable the hook MTCEVT to find muons, set the variable FULL_MTC= *.TRUE.* in MTC.RCP. To describe the other input parameters, it is necessary to describe how the program works.

Briefly, the program sweeps through the calorimeter's outermost hadronic layers, looking for contiguously hit calorimeter cells extending toward the vertex. A set of such hit cells is called a 'scan segment'. At the initial 'scanning' phase, the program requires that each calorimeter scan segment have a minimum of **MTC_HFRACSCAN** fraction of hadronic layers hit. After the initial scanning, scan segment candidate tracks are scrutinized more thoroughly using a version of MTC_MUCALTRACK (the MTC μ identification utility described in the last subsection). Final candidate tracks are required to have at least **MTC_HFRACFND** fraction of hadronic layers utilized and **MTC_FRACFND** fraction of total calorimeter layers utilized.

With the default fractions, the author found a 95% track finding efficiency for monte carlo single muons in all η, ϕ regions. By setting higher MTC_HFRACSCAN, MTC_HFRACFND, and MTC_FRACFND one is selecting exclusively the highest quality tracks. The track finding efficiency may decrease, especially in some eta regions, but one will obtain a higher background rejection.

The parameters **MTC_ETAMIN** and **MTC_ETAMAX** specify the the range in the $|\eta|$ in which to look for tracks. MTC_ETAMIN should never be less than 0.0. MTC_ETAMAX should never be less than MTC_ETAMIN. By default, the MTC μ finding program looks for muons in the full range in η (during the scanning phase).

This program will find a large number of tracks in the high η region because of the high population of hit cells at high η due to beam jet and beam halo effects. Therefore, I recommend setting MTC_ETAMAX $\leq 3.$ unless one is specifically interested in the high η region.

Final track candidates are stored in a common block MTC_FIND as defined in D0$INC:MTC_FIND.INC as shown here.

```
COMMON /MTC_FIND/
        IMTC_FULL, IMTC_NFND, IMTC_IPSTATUS, IMTC_IERROR,
        XMTC_VTXFND(3), XMTC_DVTXFND(3),
        XMTC_ETAMIN, XMTC_ETAMAX,
        XMTC_HFRACSCAN,XMTC_HFRACFND,XMTC_FRACFND,
        XMTC_TRESVFND(200),
        XMTC_FRAFND(200),XMTC_HFRAFND(200),
        XMTC_ETAFND(200),XMTC_PHIFND(200),
        XMTC_ENEFND(200)
```

The definitions of the variables stored in MTC_FIND are listed below.

PROGRAM CONTROL

The following variables are initialized with the corresponding MTC.RCP input. Their values are stored here to enable the user to change them on an event by event basis.

IMTC_FULL - set to -1 if FULL_MTC=.TRUE. in MTC.RCP. To disable (track finding) MTCEVT during your job, set IMTC_FULL to 0.

XMTC_ETAMIN - minimum $|\eta|$ in which to scan for tracks

XMTC_ETAMAX - maximum $|\eta|$ in which to scan for tracks

XMTC_HFRACSCAN - minimum fraction of hadronic layers hit required in initial MTC track scanning

XMTC_HFRACFND - minimum fraction of hadronic layers hit required in MTC track finding

XMTC_FRACFND - minimum fraction of total layers hit required in MTC track finding

IMTC_IPSTATUS - set to 0 to print status messages, set to non-zero value to stop status messages from printing

VERTEX INFORMATION

XMTC_VTXFND(3) - event vertex position in x,y,z. By default, the first event vertex from a call to ZVERT is used. If a different input vertex is desired then create a local version of MTCEVT and change the vertex definition section.

XMTC_DVTXFND(3) - uncertainty in event vertex position. By default, this uncertainty is also obtained from ZVERT.

MTC μ FINDING OUTPUT TRACKS

IMTC_IERROR - μ finding status flag is 0 if MTC track finding was successful, -1 if t[illegible] finding was unsuccessful, -1 if too many tracks were found

IMTC_NFND - number of tracks found (maximum 200)

XMTC_ETAFND(i) - η of ith calorimeter track fit (using the vertex in the fit)

XMTC_PHIFND(i) - ϕ of ith calorimeter track fit (using the vertex in the fit)

XMTC_ENEFND(i) - energy associated with the ith track

XMTC_FRAFND(i) - fraction of layers utilized with nonzero energy for ith track

XMTC_HFRAFND(i) - fraction of hadronic layers used with nonzero energy for ith track

XMTC_TRESVFND(i) - track residual of ith track

There is a limit to the number of tracks that can be found. If more than 200 tracks are found for any event, the scanning fraction, MTC_HFRACSCAN, increases incrementally so that only the best tracks are stored. When this condition occurs, if MTC_IPSTATUS is 0, status messages will be printed to the log file as MTC_HFRACSCAN is increased. If MTC_HFRACSCAN becomes = 1. (upper limit) then IMTC_IERROR is set to -1, indicating too many tracks found.

4 The Energy χ^2 Method

The energy χ^2 method has proven to be an excellent way to identify isolated muons in the calorimeter. To describe the method, if is first necessary to consider how we expect muons to deposit energy in the calorimeter.

4.1 Muon Energy deposition in the Calorimeter

The energy deposited by a muon in a liquid argon calorimeter cell depends on the number of argon gaps traversed, the thickness of the argon gaps and the energy and angle of the muon in the gap.

In the D0 calorimeter, the number of gaps, thickness of gaps, and angle of traversal of muons from the vertex varies with

- calorimeter section (there are 10 calorimeter sections: CCEM, ECEM, CCMG, ICD, ECMG, CCFH, ECIH, ECMH, CCCH, ECOH),
- calorimeter section layer number (the above 10 calorimeter sections have 4, 4, 1, 1, 1, 3, 5, 5, 1, and 3 layers, respectively), and
- η (pseudorapidity).

The distribution of energies deposited by muons in each of these calorimeter cell types has been measured in the D0 Test Beam.

Ionization is the principle form of energy loss for muons traversing a medium. δ ray emission and bremsstrahlung occur at a lower rate than basic ionization, but become more probable at higher muon energy. Figure 1 a)-b) shows the measured distribution of muon energy deposited by Test Beam muons at 15 and 50GeV in a calorimeter cell in calorimeter section ECOH layer 17, at $\eta = 1.05$. Similarly, Figure 1 c) and d) shows energy distributions for ECOH layer 17 $\eta = 1.25$ for Test Beam muons at 50 and 100GeV, respectively. In addition, Figure 1 e) and f) show analogous distributions for a cell in ECOH layer 15 at $\eta = 1.35$ for beam momenta 50 and 150 GeV, respectively.

No discernable shift in the spectrum is seen due to the change in muon energy. Only a slight increase in the population in the high tail of the distribution is observed. Therefore, we expect little variation in the calorimeter muon identification results as a function of muon energy.

Figures 2, 3, 4, and 5 show the muon energy distribution measured in calorimeter cells in the CCMG, ECMG, ECMH layer 11, and ECOH layer 16, respectively. The cell is specified by the calorimeter section, layer number and eta as given in the title. Ideally, the energy deposited in a layer of material by a muon varies according to a Landau [1] distribution. For all calorimeter cells in the Massless Gaps, the MH and the OH, this distribution was fit to a Moyal [2] function convoluted with a gaussian resolution to obtain the MPV (Most Probable Value) of the distribution. Also for each distribution, the gaussian width (σ) was also measured. These constants are used in the χ^2 calculation described in the next section.

For the CCEM, CC hadronic, ECEM and ECIH, similar distributions were available only for a single value of η as shown in Figures 6, 7, 8, and 9, respectively. This distribution was fit similarly, and the fit results for the MPV and σ obtained are used for cells at all η in that calorimeter section and layer number.

[1] A Landau distribution has a narrow peak at low values and a long asymmetric tail at high values.

[2] A Moyal function is an analytic approximation of the Landau distribution.

Table 1 displays the MPV (converted from ADC counts to GeV) obtained from this method for all calorimeter cell types listed by calorimeter section, layer number, and η. Table 2 shows the corresponding widths (in GeV).

The distributions above are the energies deposited in the cells directly in the path of the muon. Similar distributions (not shown) were plotted that included the energy of the hit cell plus the energies of all cells within .1 in η and .1 in ϕ of the hit cell in each layer (a 3×3 array of cells in each layer). These distributions were similarly fitted as above to find the characteristic MPV and σ for each cell type. The MPVs and σs obtained for these distributions are shown in Table 3 and Table 4, respectively.

4.2 Calculating the χ^2

The MPVs and widths of the distributions described in the last subsection are used to obtain a measure of muon isolation, which is analogous to the χ^2 usually defined for normal distributions. Given the direction of a candidate muon through the calorimeter, the χ^2 is defined as

$$\chi^2 = \left[\sum_{i=1}^{N_{layers}} \left(\frac{(E_i - \mu_i)^2}{\sigma_i^2} \right) \right] / N_{layers}$$

where

the sum is over all layers (N_{layers}) in the calorimeter with a hit cell in the path of the muon candidate,
E_i is the energy seen in layer i,
μ_i is the MPV of the energy for a calorimeter cell at that layer and η, and
σ_i is the width of the energy distribution for a calorimeter cell at that layer and η.

Ideally, isolated muons will be characterized by a low χ^2 and a high fraction of layers hit in the road surrounding the muon.

The χ^2 depends on the size of the calorimeter road chosen about candidate muon. If one is looking for only isolated muons, then a larger sized road will give a better measure of isolation. On the other hand, for physics topics involving a muon associated with a more energetic object close to the muon, then a χ^2 measured in a narrower road is more appropriate.

As described previously, the MTC μ identification utility calculates a number of χ^2s for different road sizes in anticipation of the different needs of the various physics analyses.

The first is the 'track χ^2' which uses only the energy in the calorimeter cells used to reconstruct the best calorimeter track segment. The MPVs and σs from Tables 1 and 2 are used for this χ^2 calculation.

The '3×3 tower χ^2' uses the energy in the cells directly in the path of the candidate muon plus the energy in all cells within .1 in η and .1 in ϕ about the central tower (a 3×3 array of cells is used in each layer). The MPVs and σs from Tables 3 and 4 are used for this χ^2 calculation. This χ^2 is an excellent measure of muon isolation. It does require, however, that the true muon location in the calorimeter is within .1 in η and ϕ of the input candidate muon direction.

Similarly, the '5×5 tower χ^2' uses the energy in the cells directly in the path of the candidate muon plus the energy in all cells within .2 in η and .2 in ϕ about the central tower (a 5×5 array of cells is used in each layer). The MPVs and σs from Tables 3 and 4 are used for this χ^2 calculation. I have found this tower size too large for a useful χ^2 calculation, but perhaps it may become useful in the future.

4.3 Applying the χ^2 method to data

The χ^2 can be used to identify isolated muons and to discriminate between muonlike objects and nonmuonlike objects in the calorimeter. To demonstrate the method, the χ^2 measurement was applied to a number of various objects in a real data sample, namely the $t \rightarrow e\mu$ final candidate sample. The 713 events in this sample contain a total of

957	muons in the PMUO bank,
810	electrons in the PELC bank, and
1445	jets in the JETS bank

without offline cuts.

I chose this sample because it is a very well studied sample that is known to contain very nearly one well measured (real) muon per event. For all electrons, muons and jets in the banks, I calculated the χ^2 and the fraction of layers hit in a calorimeter tower extending .3 in η and .3 in ϕ centered on the object in question. The resulting χ^2 versus the fraction of layers hit for electrons, muon and jets is shown in Figure 10 a), b), and c), respectively.

Ideal MIPs (Minimum Ionizing Particles) will be characterized by a low χ^2 and a high fraction of layers hit. In the figure, a large fraction of the muons in the sample have this characteristic, while the electrons and jets do not. The electrons and jets typically have a lower fraction of layers hit and a higher χ^2. This demonstrates clearly the power of the χ^2 method in distinguishing single penetrating particles from other objects.

Muons are expected to be more isolated in the hadronic section than in the electromagnetic section from low energy particle scattering. So, similarly, one can measure a χ^2 and fraction of layers hit exclusively in the hadronic section for each of these objects. The results are shown in Figure 11 a), b) and c), for electrons, muons and jets, respectively. In this case, over half of the muons in the sample have an energy deposition in the hadronic section of the calorimeter characteristic of an ideal isolated MIP. Again, electrons and jets generally have a smaller fraction of layers hit and a higher χ^2.

The χ^2 can also be used to measure when a muon emerges from a more energetic object as described in an earlier section. The track χ^2 (Equation 4.2) is the sum of χ^2 terms measured in each layer divided by the number of layers. The muon is said to emerge at the layer in which the terms in the χ^2 beyond that layer are characteristically small (indicating single particle traversal). The MTC μ identification package output includes a word indicating the layer at which the muon seems to separate from a more energetic object. Also, the χ^2 beyond that layer is included in the output bank, as described earlier.

5 Tracking Muons in the Calorimeter

The MTC μ identification program and the MTC μ finding program provide calorimeter track muon segments in their output. This section describes how the best track segment is found. I define a 'hit' cell as any calorimeter cell with a positive energy above zero suppression.

Both MTC programs use an input vertex position, η and ϕ of the track candidate(s):

- The identification program is called with an input vertex position, η and ϕ of the track candidate.
- The finding program uses the primary event vertex from the vertex bank. In an initial scanning phase, candidate tracks are located by finding sets of contiguously hit cells in the hadronic section which extend toward the vertex. The η and ϕ locations of these track candidates are then the input to the track finding program.

Given the input vertex position, η and ϕ of each track candidate, the program first finds the calorimeter cells along that candidate's trajectory in each layer. I call this set of cells the **'central tower'**. The program then identifies all the calorimeter cells within .2 in η and .2 in ϕ from the central tower (if they exist). This road is called the '5×5 **tower**' because it contains a 5×5 square array of cells in each layer (a total of 25 calorimeter cells in each layer).

The best calorimeter muon track is found by fitting a line through the longest set of contiguously hit calorimeter cells projected from the hadronic section toward the vertex in the 5×5 tower. This method exploits the properties that

- penetrating objects will be most isolated in the hadronic section of the calorimeter,
- muon tracks are straight in the calorimeter, and
- muons generally emerge from a known (vertex) point.

Two fits were done for the best set of calorimeter points, one uses only the calorimeter points the other includes the vertex in the fit.

The calorimeter points used in the fit are the (x, y, z) coordinates of the volume weighted mean position of each hit cell (obtained using D0 routine CELXYZ). A weighted linear fit (LFITW from the CERN library) was used to obtain the best fit line independently in the (x, z) and (y, z) planes. The weight assigned to the vertex point is the inverse square of the uncertainty in the z vertex coordinate. The weights for the calorimeter points were the inverse square of half the cell size in the z direction. Table 5 shows the longitudinal calorimeter cell size in centimeters listed by calorimeter layer number and η.

Fits in the (x, z) and (y, z) planes were combined to get the best fit in 3-dimensional space. Track residuals, the square root of the sum of the squares of the residuals of the fitted points from the fit line, are stored in the MTC output common block along with the fit results.

Hot cells (discharge) and calorimeter (electronics or uranium) noise are not expected to greatly influence track finding since these effects should not be, in general, correlated layer by layer. The following two subsections describe the calorimeter track finding efficiencies and resolution.

The ideal track verification efficiency, calorimeter tracking resolution, and track finding efficiency can be studied using Monte Carlo (MC) single muon events. There are two type of MC single muon files which I used for these studies.

1. 500 Monte Carlo single muons were generated at 6 discrete η values (listed below) with $\phi = 0$ and a vertex position at $(x, y, z) = (0, 0, 0)$.

   (a) $\eta = 0.8125$ – 500 events

   (b) $\eta = 0.9125$ – 500 events

   (c) $\eta = 1.0125$ – 500 events

   (d) $\eta = 1.1125$ – 500 events

   (e) $\eta = 1.2125$ – 500 events

   (f) $\eta = 1.3125$ – 500 events

   These files were generated by Mark Sosebee and Kaushik De for studies of calorimeter response in the ICR (Inter Cryostat Region).

2. 10,000 Monte Carlo single muons were generated with a vertex distribution representative of that found in the real data. These muons are uniformly distributed in η and ϕ space. They were generated by the muon group for muon system studies and made available to me via Thorsten Huehn.

These files are used in the next few subsections to demonstrate ideal MTC efficiencies and tracking resolution.

5.1 Track Verification Efficiency

For the reconstructed MC muon samples at discrete η, muons from the PMUO bank were used as input candidate tracks to the MTC μ identification utility. The input vertex position was the reconstructed event vertex. The MTC utility verified nearly 100% of all input tracks.

For the reconstructed MC muon samples distributed uniformly in η and ϕ, again, muons from the PMUO bank were used as input candidate tracks and the reconstructed event vertex was used as the input vertex position. The MTC μ identification utility verified over 96% of the input tracks. This efficiency is constant as a function of η or ϕ.

The slight decrease in track verification efficiency is due to the difference in the vertex distribution of the Monte Carlo files: the discrete η muon samples were generated with a vertex at $z = 0$ (reconstructed vertices were generally between $z = -10$ and 10 cm), while the vertex distribution of the latter sample was centered at 0 with a wider distribution more representative of real data (the reconstructed vertex position ranged between $z = -60$ to 60 cm). Therefore, the MTC package track verification efficiency is slightly degraded (at a less than a 5% level) in events with a combined non-projective geometry (z vertex position nonzero) and vertex position reconstruction uncertainty.

5.2 Tracking Resolution

The spatial resolution of calorimeter tracks found is dominated by the calorimeter segmentation, which is, in general, 0.1 in pseudorapidity (eta) and polar angle (phi).

The scatterplot in Figures 12, 13, 14, 15, 16 and 17 shows the reconstructed η of the muon system versus the reconstructed η of the calorimeter for the 6 MC muon samples at discrete η (at η=0.8125, 0.9125, 1.0125, 1.1125, 1.2125 and 1.3125, respectively). Plots b) and c) in these figures show the projections of this scatterplot to show the muon tracking resolution and the calorimeter tracking resolution, for comparison. The calorimeter tracking was obtained using the MTC μ identification utility using muons from the PMUO bank as input candidate tracks and the reconstructed event vertex as the input vertex position.

The distribution is notably wider for the calorimeter tracking case, as expected from the broader calorimeter segmentation. Clearly the tracking resolution is better in the muon system. No cuts were applied to the PMUO muon track quality. The RMS of these distributions is comparable only because of the outliers in the muon tracking distribution. The point in showing the outliers is to show that for these tracks, despite the poor muon system tracking for these tracks, the calorimeter tracking finds the proper location of the muon within .1 in η in all cases. The current global fit includes muon track and central detector muon track matching only. These results indicate that adding calorimeter tracking to the global fitting of muons through the detector may be beneficial.

For the MC muon sample with muons distributed uniformly in η,ϕ space, Figure 18 a) shows the reconstructed η of the muon system versus the reconstructed η of the calorimeter. The tracking resolution is best in the central η region, worsening with increasing pseudorapidity.

Also for this MC muon sample, Figure 18 b) shows the reconstructed ϕ of the muon system versus the reconstructed ϕ of the calorimeter. Tracking resolution seems to be constant in ϕ. The bunching structure seen in this plot is caused by the calorimeter cell size: there are 10 calorimeter cells per unit ϕ, thus there are 10 bunches in the plot per unit ϕ.

For the muons in the $t \rightarrow e\mu$ final candidate sample, Figure 19 a) shows the reconstructed η of the muon system versus the reconstructed η of the calorimeter for 691 muon tracks verified in the calorimeter. A calorimeter track is considered good if the fraction of hadronic layers utilized was greater than .65. There are approximately 713 known good tracks in the sample, so the MTC muon verification efficiency for this set of cuts is about 97%. Figure 19 b) shows the reconstructed ϕ of the muon system versus the reconstructed ϕ of the calorimeter for this sample.

5.3 Track Finding Efficiency

For the reconstructed MC muon samples at discrete η, the MTC μ finding utility uses the first reconstructed event vertex as input. The muon system μ finding efficiency varied between 94 and 99% for this sample (there are no gaps in coverage in the muon system at $\phi = 0.$). MTC μ finding efficiency also ranges from 94 to 100% for all these files at discrete η.

For the reconstructed MC muon sample with muons distributed uniformly in η and ϕ, again, the reconstructed event vertex was used as the input vertex position. The MTC μ finding efficiency was 95% for this sample. The corresponding muon system μ finding efficiency was about 69%.

Of the total 10,000 muons in the sample, 6528 tracks were found by both the muon system and the calorimeter. Figure 20 a) shows the reconstructed η of the muon system versus the reconstructed η of the calorimeter and Figure 20 b) shows the corresponding ϕ plot for all 'matched tracks' found. A calorimeter track is 'matched' to a muon track if the calorimeter track lies within a cone size of approximately .5 of a muon track.

Figure 21 a) shows the distribution of the MTC found muons in η, ϕ space. Figure 21 b) and c) show the corresponding projections in η and ϕ. Both the projections are flat indicating the the MTC μ finding program μ finding efficiency is constant in in η and ϕ. No gaps in coverage are observed.

Figure 22 a) shows the η, ϕ distribution of the muons found by the muon system (in the PMUO bank). Figure 22 b) and c) show the corresponding projections in η and ϕ. The sparsely populated areas in Figure 22 a) show the regions of known muon system μ finding inefficiency. It is hoped that the MTC μ finding utility can be used to enhance the overall D0 detector muon finding efficiency.

For the muons in the $t \rightarrow e\mu$ final candidate sample, Figure 23 a) and b) shows the number of muons found by the muon system and the MTC μ finding program, respectively. Although the MTC program finds a large number of tracks, over 83% of those tracks found have an $\eta \geq 3.0$. This high number of tracks in the high eta region is expected due to beam jet and beam halo effects.

Figure 24 a) shows the η, ϕ distribution of the muons found by the MTC program. Figures 24 b) and c) show the projections of this scatterplot. From Figure 24 b), the sharp rise in the number of tracks found occurs around $\eta = 3.0$.

Figure 25 a) and b) shows the number of muons found by the muon system and the MTC μ finding program, respectively, in the restricted η range from -2.0 to 2.0. The MTC.RCP input parameters to obtain this level of rejection was MTC_HFRACSCAN = 0.57, MTC_HFRACFND = 0.66, and MTC_FRACFND = 0.50. An average of just over 3 tracks per event was found in this η range, with a high correlation between tracks found by MTC with those found in the muon system. A higher background rejection is possible by raising the last two fractions.

6 Conclusions

Currently, a number of physics analyses are using the package for fake muon rejection, vertex confirmation, and ruling out the presence of a muon in a given direction. The information provided by the MTC package has a much higher efficiency for muon identification and background rejection than the 'calorimeter confirmation' energy sum [3] which contains no mechanism for the pattern recognition of tracks.

Work is in progress to incorporate calorimeter tracking into the global muon fitting and to use the MTC μ finding program to check muon system efficiencies.

We know that the D0 calorimeter is an excellent device for measuring energy. Its segmentation, uniform coverage, and density also make it useful for identifying penetrating particles traveling through it. This calorimeter track recognition is made possible using the MTC package.

7 Acknowledgements

There are a number of individuals who have assisted me in this project with either ideas, criticisms, data files, help in running D0 software and help in the debugging process. Specifically, I'd most like to thank Daria Zieminska, Gene Alvarez, Terry Geld, Kaushik De, Mark Sosebee, Thorsten Huehn, Dharmaratna Welanthantri, John Balderston, Jim Cochran, Richard Astur, Jonathan Kotcher, John Womersley, Jim Jaques, Cecilia Gerber, and Dan Owen for their input.

[3] The calorimeter confirmation energy sum is a simple sum of the calorimeter energy seen about candidate tracks.

Table 1: MPV (Most Probable Value) of energy deposited by muons in each calorimter cell type. MPVs are listed by layer number (ILYR) and ieta ($I\eta$) from fitted distributions for each cell type from the D0 Test Beam.

MPV by layer number (ILYR) and η (IETA) in GeV																	
	ILYR																
$I\eta$	1	2	3	4	5	6	7	8	9	10	11	12	13	14	15	16	17
37	–	–	–	–	–	–	–	–	–	–	–	–	353	353	1061	–	–
36	–	–	–	–	–	–	–	–	–	–	382	353	353	353	1061	–	–
35	35	28	92	–	–	–	131	–	–	–	382	353	353	353	1061	–	–
34	35	28	92	–	–	–	131	–	–	–	382	353	353	353	1061	–	–
33	35	28	92	–	–	–	131				382	353	353	353	1061	–	–
32	35	28	92	–	–	–	131	–	–	–	382	353	353	353	1061	–	–
31	35	28	92	–	–	–	131	–	–	–	382	353	353	353	1061	–	–
30	35	28	92	–	–	–	131	–	–	–	382	353	353	353	1061	–	–
29	35	28	92	–	–	–	131	–	–	–	382	353	353	353	1061	–	–
28	35	28	92	–	–	–	131		–	–	382	353	353	353	1061	–	–
27	35	28	92	–	–	–	131	–	–	–	382	353	353	353	1061	–	–
26	35	28	92	92	92	92	131	–	–	–	382	353	353	353	1061	–	–
25	35	28	92	92	92	92	131	–	–	–	382	353	353	353	1061	–	–
24	35	28	92	92	92	92	131	–	–	–	382	353	353	353	1061	–	–
23	35	28	92	92	92	92	131	–	–	–	382	353	353	353	1061	–	–
22	35	28	92	92	92	92	131	–	–	–	382	353	353	353	707	–	–
21	35	28	92	92	92	92	131	–	–	–	382	353	353	353	354	–	–
20	35	28	92	92	92	92	131	–	–	–	382	353	353	176	415	–	–
19	35	28	92	92	92	92	131	–	–	–	382	353	176	–	623	–	–
18	35	28	92	92	92	92	131	–	–	–	382	176	–	374	623	–	–
17	35	28	92	92	92	92	131	–	–	–	191	182	374	374	623	–	–
16	35	28	92	92	92	92	131	–	–	–	392	363	374	374	623	–	–
15	35	28	92	92	92	92	131	–	–	–	392	363	374	374	415	–	–
14	–	–	–	–	92	92	131	–	66	–	392	363	374	374	208	–	194
13	–	–	–	–	–	–	–	–	101	86	408	373	355	0	–	154	200
12	25	16	80	80	–	–	–	192	80	151	444	201	–	–	62	212	200
11	25	16	80	80	80	80	120	138	68	113	0	–	–	–	198	200	80
10	25	16	80	80	80	80	120	187	46	89	486	–	–	–	216	137	–
9	25	16	80	80	80	80	120	153	224	59	486	346	–	–	229	0	–
8	25	16	80	80	80	80	120	137	–	240	486	346	278	–	114	–	–
7	25	16	80	80	80	80	120	–	–	–	486	346	278	–	–	–	–
6	25	16	80	80	80	80	120	–	–	–	486	346	278	–	1012	–	–
5	25	16	80	80	80	80	120	–	–	–	486	346	278	–	1012	–	–
4	25	16	80	80	80	80	120	–	–	–	486	346	278	–	1012	–	–
3	25	16	80	80	80	80	120	–	–	–	486	346	278	–	1012	–	–
2	25	16	80	80	80	80	120	–	–	–	486	346	278	–	1012	–	–
1	25	16	80	80	80	80	120	–	–	–	486	346	278	–	1012	–	–

Table 2: Gaussian width of the distribution of energy deposited by muons in each calorimter cell type. MPVs are listed by layer number (ILYR) and ieta ($I\eta$) from fitted distributions for each cell type from the D0 Test Beam.

MPV by layer number (ILYR) and η (IETA) in GeV

	ILYR																
$I\eta$	1	2	3	4	5	6	7	8	9	10	11	12	13	14	15	16	17
37	–	–	–	–	–	–	–	–	–	–	–	–	172	172	476	–	–
36	–	–	–	–	–	–	–	–	–	–	186	172	172	172	476	–	–
35	27	18	63	–	–	–	69	–	–	–	186	172	172	172	476	–	–
34	27	18	63	–		–	69	–	–	–	186	172	172	172	476	–	–
33	27	18	63	–	–	–	69	–	–		186	172	172	172	476	–	–
32	27	18	63	–	–	–	69	–	–	–	186	172	172	172	476	–	–
31	27	18	63	–	–		69	–	–	–	186	172	172	172	476	–	–
30	27	18	63	–	–	–	69	–	–	–	186	172	172	172	476	–	–
29	27	18	63	–	–	–	69	–	–	–	186	172	172	172	476	–	–
28	27	18	63	–	–	–	69	–	–	–	186	172	172	172	476	–	–
27	27	18	63	–	–		69	–	–		186	172	172	172	476	–	–
26	27	18	63	63	63	63	69	–		–	186	172	172	172	476	–	–
25	27	18	63	63	63	63	69	–	–	–	186	172	172	172	476		–
24	27	18	63	63	63	63	69	–	–	–	186	172	172	172	476	–	–
23	27	18	63	63	63	63	69	–	–	–	186	172	172	172	476	–	–
22	27	18	63	63	63	63	69	–	–	–	186	172	172	172	476	–	–
21	27	18	63	63	63	63	69	–		–	186	172	172	172	476	–	–
20	27	18	63	63	63	63	69	–	–	–	186	172	172	172	282	–	–
19	27	18	63	63	63	63	69	–	–	–	186	172	172	–	282	–	–
18	27	18	63	63	63	63	69	–	–		186	172	–	149	282	–	–
17	27	18	63	63	63	63	69	–	–	–	186	143	149	149	282	–	–
16	27	18	63	63	63	63	69		–	–	162	143	149	149	282	–	–
15	27	18	63	63	63	63	69	–	–	–	162	143	149	149	282	–	–
14	–	–	–	–	63	63	69	–	17	–	162	143	149	149	282	–	114
13	–	–	–	–	–	–	–	–	25	128	167	153	153	110	–	109	120
12	31	20	59	59	–	–	–	260	20	240	167	162	–	–	87	120	126
11	31	20	59	59	59	59	87	212	22	147	115	–	–	–	130	120	97
10	31	20	59	59	59	59	87	253	15	144	245	–	–	–	130	109	–
9	31	20	59	59	59	59	87	359	74	148	245	234	–	–	167	63	–
8	31	20	59	59	59	59	87	323	–	599	245	234	208	–	167	–	–
7	31	20	59	59	59	59	87	–	–	–	245	234	208	–	–	–	–
6	31	20	59	59	59	59	87	–	–	–	245	234	208	–	469	–	–
5	31	20	59	59	59	59	87	–	–	–	245	234	208	–	469	–	–
4	31	20	59	59	59	59	87	–	–	–	245	234	208	–	469	–	–
3	31	20	59	59	59	59	87	–	–	–	245	234	208	–	469	–	–
2	31	20	59	59	59	59	87		–	–	245	234	208	–	469	–	–
1	31	20	59	59	59	59	87	–	–	–	245	234	208	–	469	–	–

Table 3: MPV (Most Probable Value) of energy deposited by muons in each calorimter cell type. MPVs are listed by layer number (ILYR) and ieta ($I\eta$) from fitted distributions for each cell type from the D0 Test Beam. The energy distribution includes energy deposited in the hit cell plus any deposited in all cells within .1 in η and .1 in ϕ from the hit cell in each layer.

MPV by layer number (ILYR) and η (IETA) in GeV																	
	ILYR																
$I\eta$	1	2	3	4	5	6	7	8	9	10	11	12	13	14	15	16	17
37	–	–	–	–	–	–	–	–	–			–	353	353	1061	–	–
36	–	–	–	–	–	–	–	–	–	–	382	353	353	353	1061	–	–
35	35	28	92	–	–	–	131		–	–	382	353	353	353	1061	–	–
34	35	28	92	–	–	–	131	–	–	–	382	353	353	353	1061	–	–
33	35	28	92	–	–	–	131		–	–	382	353	353	353	1061	–	–
32	35	28	92	–	–	–	131	–	–		382	353	353	353	1061	–	–
31	35	28	92	–	–	–	131	–	–	–	382	353	353	353	1061	–	–
30	35	28	92	–	–	–	131		–	–	382	353	353	353	1061	–	–
29	35	28	92	–	–	–	131	–	–	–	382	353	353	353	1061	–	–
28	35	28	92	–	–	–	131	–	–	–	382	353	353	353	1061	–	–
27	35	28	92	–	–	–	131	–			382	353	353	353	1061	–	–
26	35	28	92	92	92	92	131	–	–	–	382	353	353	353	1061	–	–
25	35	28	92	92	92	92	131				382	353	353	353	1061	–	–
24	35	28	92	92	92	92	131	–	–	–	382	353	353	353	1061	–	–
23	35	28	92	92	92	92	131	–	–	–	382	353	353	353	1061	–	–
22	35	28	92	92	92	92	131	–	–	–	382	353	353	353	707	–	–
21	35	28	92	92	92	92	131	–	–	–	382	353	353	353	354	–	–
20	35	28	92	92	92	92	131	–	–	–	382	353	353	176	484	–	–
19	35	28	92	92	92	92	131	–	–	–	382	353	176	–	746	–	–
18	35	28	92	92	92	92	131				382	176	–	374	746	–	–
17	35	28	92	92	92	92	131	–	–	–	191	205	393	374	746	–	–
16	35	28	92	92	92	92	131	–	–	–	429	406	393	374	746	–	–
15	35	28	92	92	92	92	131	–	–	–	429	406	393	374	484	–	–
14	–	–	–	–	92	92	131	–	66	–	429	406	393	374	242	–	200
13	–	–	–	–	–	–		–	119	85	434	401	364	0	–	149	206
12	25	16	80	80	–	–	–	203	73	179	481	225	–	–	80	223	212
11	25	16	80	80	80	80	120	175	75	103	0	–	–	–	204	206	86
10	25	16	80	80	80	80	120	192	63	99	486	–	–	–	216	132	–
9	25	16	80	80	80	80	120	153	312	82	486	346	–	–	216	30	–
8	25	16	80	80	80	80	120	137	–	333	486	346	278	–	111	–	–
7	25	16	80	80	80	80	120	–	–	–	486	346	278	–	–	–	–
6	25	16	80	80	80	80	120	–	–	–	486	346	278	–	1012	–	–
5	25	16	80	80	80	80	120	–	–	–	486	346	278	–	1012	–	–
4	25	16	80	80	80	80	120	–	–	–	486	346	278	–	1012	–	–
3	25	16	80	80	80	80	120	–	–	–	486	346	278	–	1012	–	–
2	25	16	80	80	80	80	120	–	–	–	486	346	278	–	1012	–	–
1	25	16	80	80	80	80	120	–	–	–	486	346	278	–	1012	–	–

Table 4: Gaussian width of the distribution of energy deposited by muons in each calorimter cell type. MPVs are listed by layer number (ILYR) and IETA ($I\eta$) from fitted distributions for each cell type from the D0 Test Beam. The energy distribution includes energy deposited in the hit cell plus any deposited in all cells within .1 in η and .1 in ϕ from the hit cell in each layer.

MPV by layer number (ILYR) and η (IETA) in GeV																	
	ILYR																
$I\eta$	1	2	3	4	5	6	7	8	9	10	11	12	13	14	15	16	17
37	–	–	–	–	–	–	–	–	–	–	–	–	172	172	476	–	–
36	–	–	–	–	–	–	–	–	–	–	186	172	172	172	476	–	–
35	27	18	63	–	–	–	69	–	–		186	172	172	172	476	–	–
34	27	18	63	–	–	–	69	–	–	–	186	172	172	172	476	–	–
33	27	18	63	–	–	–	69	–	–	–	186	172	172	172	476	–	–
32	27	18	63	–	–	–	69	–	–	–	186	172	172	172	476	–	–
31	27	18	63	–	–		69	–	–	–	186	172	172	172	476	–	–
30	27	18	63	–	–	–	69	–	–	–	186	172	172	172	476	–	–
29	27	18	63		–	–	69	–	–	–	186	172	172	172	476	–	–
28	27	18	63	–	–	–	69	–	–	–	186	172	172	172	476	–	–
27	27	18	63	–	–	–	69	–	–	–	186	172	172	172	476	–	–
26	27	18	63	63	63	63	69	–	–		186	172	172	172	476	–	
25	27	18	63	63	63	63	69	–	–		186	172	172	172	476	–	–
24	27	18	63	63	63	63	69	–	–	–	186	172	172	172	476	–	–
23	27	18	63	63	63	63	69	–	–	–	186	172	172	172	476	–	–
22	27	18	63	63	63	63	69	–	–	–	186	172	172	172	476	–	–
21	27	18	63	63	63	63	69	–	–	–	186	172	172	172	476	–	–
20	27	18	63	63	63	63	69	–	–	–	186	172	172	172	343	–	–
19	27	18	63	63	63	63	69	–	–	–	186	172	172	–	343	–	–
18	27	18	63	63	63	63	69	–	–	–	186	172	–	206	343	–	–
17	27	18	63	63	63	63	69	–	–	–	186	205	211	206	343	–	–
16	27	18	63	63	63	63	69	–	–	–	225	205	211	206	343	–	–
15	27	18	63	63	63	63	69	–	–	–	225	205	211	206	343	–	–
14	–	–	–	–	63	63	69	–	16	–	225	205	211	206	343	–	126
13	–	–	–	–	–	–	–	–	30	138	235	205	206	158	–	120	137
12	31	20	59	59	–	–	–	338	18	277	220	196	–	–	105	137	137
11	31	20	59	59	59	59	87	247	25	184	162	–	–	–	142	137	109
10	31	20	59	59	59	59	87	311	21	169	245	–	–	–	142	120	–
9	31	20	59	59	59	59	87	484	103	206	245	234	–	–	179	92	–
8	31	20	59	59	59	59	87	435	–	832	245	234	208	–	179	–	–
7	31	20	59	59	59	59	87	–	–	–	245	234	208	–	–	–	–
6	31	20	59	59	59	59	87	–		–	245	234	208	–	469	–	–
5	31	20	59	59	59	59	87	–	–	–	245	234	208	–	469	–	–
4	31	20	59	59	59	59	87		–	–	245	234	208	–	469	–	–
3	31	20	59	59	59	59	87	–	–	–	245	234	208	–	469	–	–
2	31	20	59	59	59	59	87	–	–	–	245	234	208	–	469	–	–
1	31	20	59	59	59	59	87	–	–	–	245	234	208	–	469	–	–

Table 5: Longitudinal width of each calorimeter cell type listed by layer number (ILYR) and ieta ($I\eta$) in centimeters.

Longitudinal (z) size of calorimeter cells by layer number (ILYR) and η (IETA) in cm

	ILYR																
$I\eta$	1	2	3	4	5	6	7	8	9	10	11	12	13	14	15	16	17
37	-	-	-	-	-	-	-	-	-	-	-	-	24.8	22.7	71.1	-	-
36	-	-	-	-	-	-	-	-	-	-	25.5	24.8	24.8	22.7	71.1	-	-
35	2.0	2.5	7.6	-	-	-	9.6	-	-	-	25.5	24.8	24.8	22.7	71.1	-	-
34	2.0	2.5	7.6	-	-	-	9.6	-	-	-	25.5	24.8	24.8	22.7	71.1	-	-
33	2.0	2.5	7.6	-	-	-	9.6	-	-	-	25.5	24.8	24.8	22.7	71.1	-	-
32	2.0	2.5	7.6	-	-	-	9.6	-	-	-	25.5	24.8	24.8	22.7	71.1	-	-
31	2.0	2.5	7.6	-	-	-	9.6	-	-	-	25.5	24.8	24.8	22.7	71.1	-	-
30	2.0	2.5	7.6	-	-	-	9.6	-	-	-	25.5	24.8	24.8	22.7	71.1	-	-
29	2.0	2.5	7.6	-	-	-	9.6	-	-	-	25.5	24.8	24.8	22.7	71.1	-	-
28	2.0	2.5	7.6	-	-	-	9.6	-	-	-	25.5	24.8	24.8	22.7	71.1	-	-
27	2.0	2.5	7.6	-	-	-	9.6	-	-	-	25.5	24.8	24.8	22.7	71.1	-	-
26	2.0	2.5	7.6	7.6	7.6	7.6	9.6	-	-	-	25.5	24.8	24.8	22.7	71.1	-	-
25	2.0	2.5	7.6	7.6	7.6	7.6	9.6	-	-	-	25.5	24.8	24.8	22.7	71.1	-	-
24	2.0	2.5	7.6	7.6	7.6	7.6	9.6	-	-	-	25.5	24.8	24.8	22.7	71.1	-	-
23	2.0	2.5	7.6	7.6	7.6	7.6	9.6	-	-	-	25.5	24.8	24.8	22.7	71.1	-	-
22	2.0	2.5	7.6	7.6	7.6	7.6	9.6	-	-	-	25.5	24.8	24.8	22.7	71.1	-	-
21	2.0	2.5	7.6	7.6	7.6	7.6	9.6	-	-	-	25.5	24.8	24.8	22.7	27.0	-	-
20	2.0	2.5	7.6	7.6	7.6	7.6	9.6	-	-	-	25.5	24.8	24.8	22.7	78.3	-	-
19	2.0	2.5	7.6	7.6	7.6	7.6	9.6	-	-	-	25.5	24.8	11.8	-	77.8	-	-
18	2.0	2.5	7.6	7.6	7.6	7.6	9.6	-	-	-	25.5	11.8	-	17.1	77.8	-	-
17	2.0	2.5	7.6	7.6	7.6	7.6	9.6	-	-	-	12.4	17.7	17.7	17.1	77.8	-	-
16	2.0	2.5	7.6	7.6	7.6	7.6	9.6	-	-	-	17.7	17.7	17.7	17.1	77.8	-	-
15	2.0	2.5	7.6	7.6	7.6	7.6	9.6	-	-	-	17.7	17.7	17.7	17.1	77.0	-	-
14	-	-	-	-	2.5	2.5	9.6	-	20	-	17.7	17.7	17.7	17.1	25.6	-	48.4
13	-	-	-	-	-	-	-	-	20	20	17.7	17.7	17.7	8.2	-	48.4	48.4
12	15.9	13.3	7.2	7.2	-	-	-	20	20	20	17.7	17.7	-	-	48.4	48.4	48.4
11	13.7	14.0	7.2	7.2	7.5	7.5	13.1	20	20	20	8.2	-	-	-	48.4	48.4	48.4
10	12.7	13.0	6.7	6.7	6.9	6.9	14.8	20	20	20	7.4	-	-	-	48.4	48.4	-
9	11.8	12.1	6.2	6.2	6.5	6.5	13.8	20	20	20	16.4	4.4	-	-	48.4	48.4	-
8	11.1	11.3	5.8	5.8	6.0	6.0	12.9	20	-	20	15.4	18.2	9.5	-	48.4	-	-
7	10.4	10.6	5.5	5.5	5.7	5.7	12.1	-	-	-	14.5	17.2	19.3	-	-	-	-
6	9.9	10.1	5.2	5.2	5.4	5.4	11.5	-	-	-	13.7	16.3	18.3	-	25.9	-	-
5	9.4	9.6	5.0	5.0	5.1	5.1	11.0	-	-	-	13.1	15.5	17.4	-	21.5	-	-
4	9.1	9.3	4.8	4.8	4.9	4.9	10.6	-	-	-	12.6	14.9	16.8	-	20.7	-	-
3	8.8	9.0	4.7	4.7	4.8	4.8	10.3	-	-	-	12.3	14.5	16.3	-	20.1	-	-
2	8.6	8.8	4.6	4.6	4.7	4.7	10.1	-	-	-	12.0	14.2	16.0	-	19.7	-	-
1	8.6	8.7	4.6	4.6	4.6	4.6	10.0	-	-	-	11.9	14.1	15.8	-	19.5	-	-

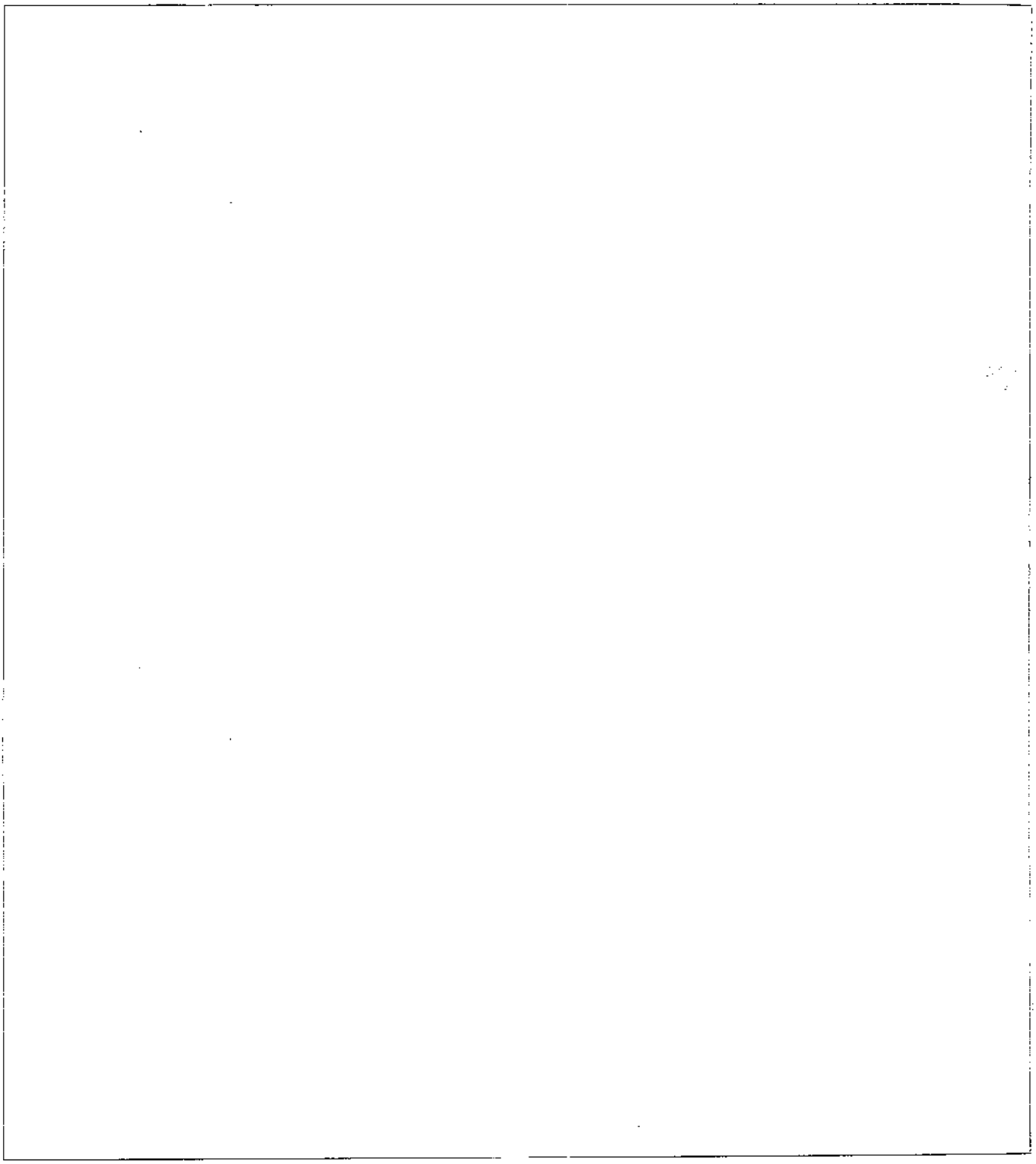

Figure 1: Distributions of energy (in ADC counts) deposited in a calorimeter cell by D0 Test Beam muons at various energies. The calorimeter cell and beam energy are as indicated below: a) ECOH layer 17 $\eta = 1.05, p_\mu = 15$GeV, b) ECOH layer 17 $\eta = 1.05, p_\mu = 50$GeV, c) ECOH layer 17 $\eta = 1.25, p_\mu = 50$GeV, d) ECOH layer 17 $\eta = 1.25, p_\mu = 100$GeV, e) ECOH layer 15 $\eta = 1.35, p_\mu = 50$GeV, and f) ECOH layer 15 $\eta = 1.35, p_\mu = 150$GeV

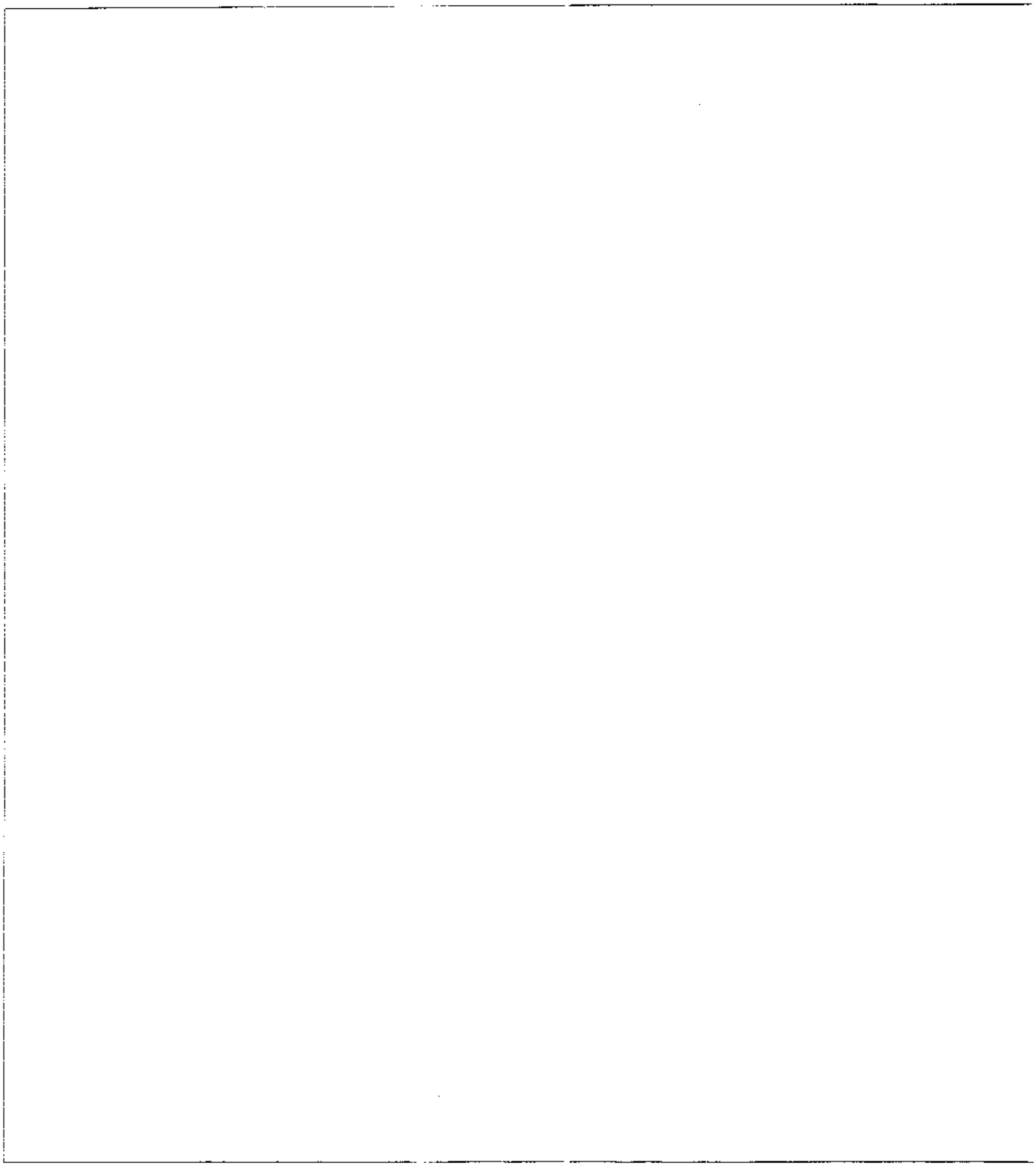

Figure 2: D0 Test Beam muon energy distribution (in ADC counts) seen in the calorimeter cells in the CCMG. The cell's η is given in each figure title.

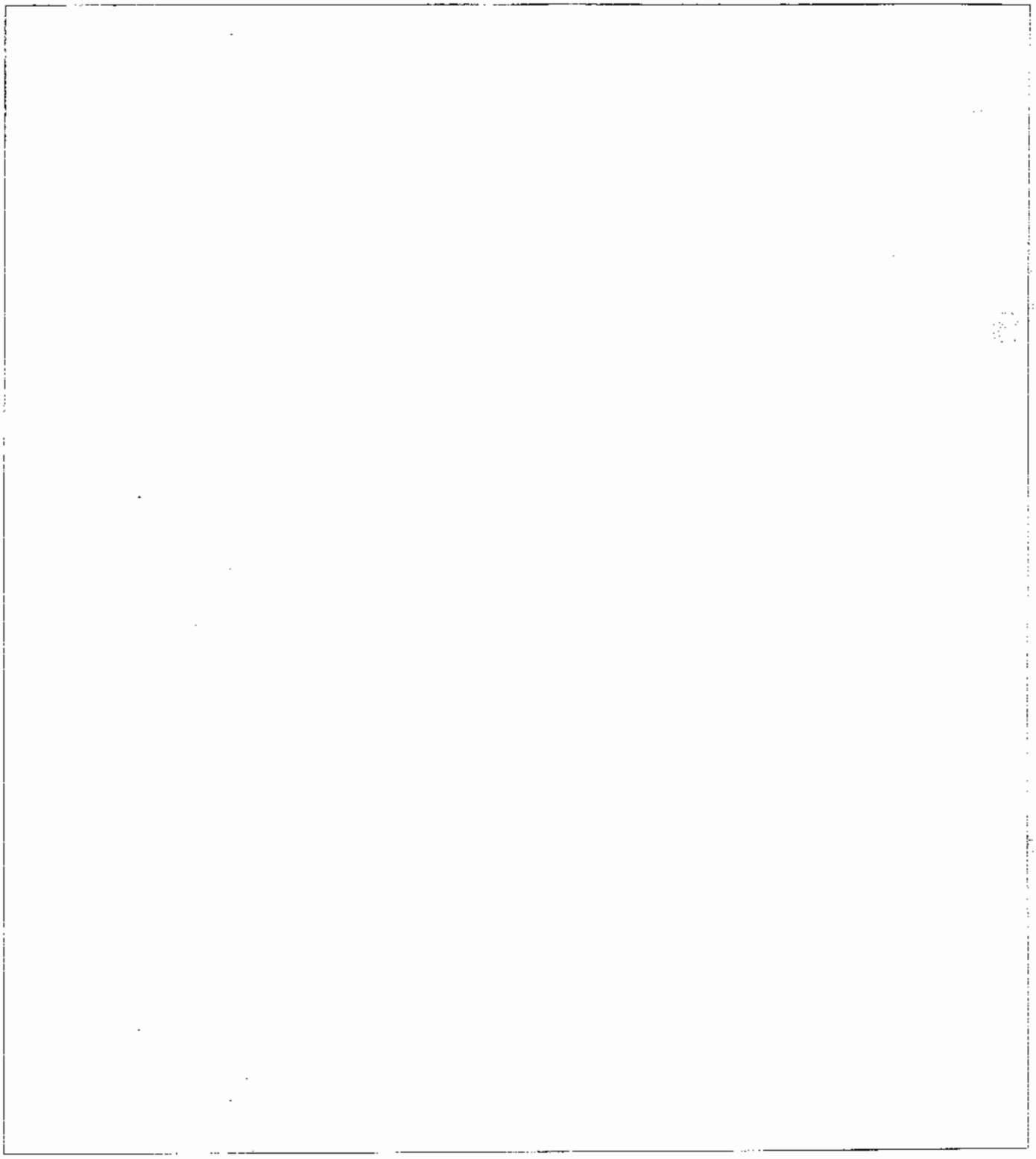

Figure 3: D0 Test Beam muon energy distribution (in ADC counts) seen in the calorimeter cells in the ECMG. The cell's η is given in each figure title.

Figure 4: D0 Test Beam muon energy distribution (in ADC counts) seen in the calorimeter cells in the ECMH layer 11. The cell's η is given in each figure title.

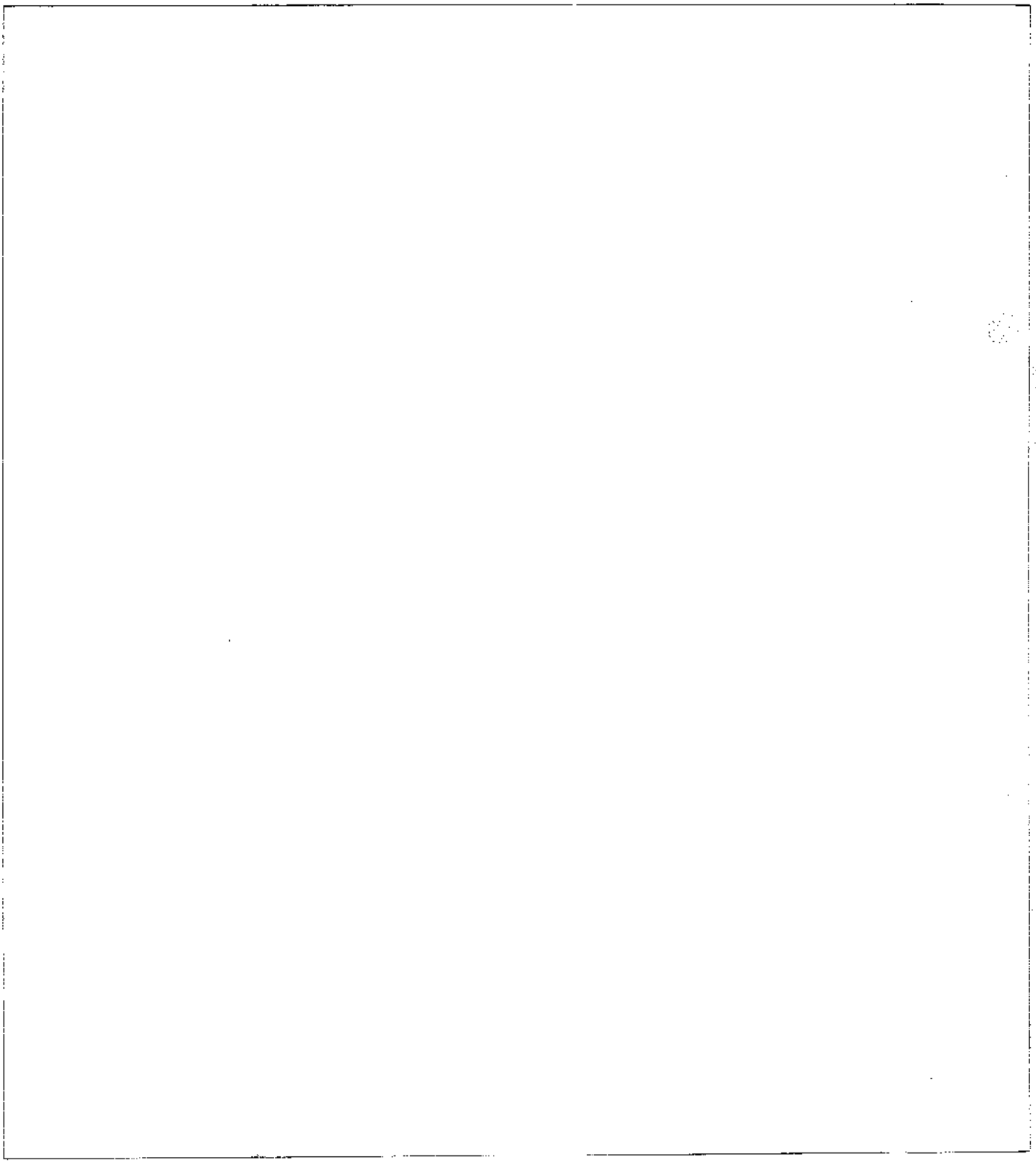

Figure 5: D0 Test Beam muon energy distribution (in ADC counts) seen in the calorimeter cells in the ECOH layer 16. The cell's η is given in each figure title.

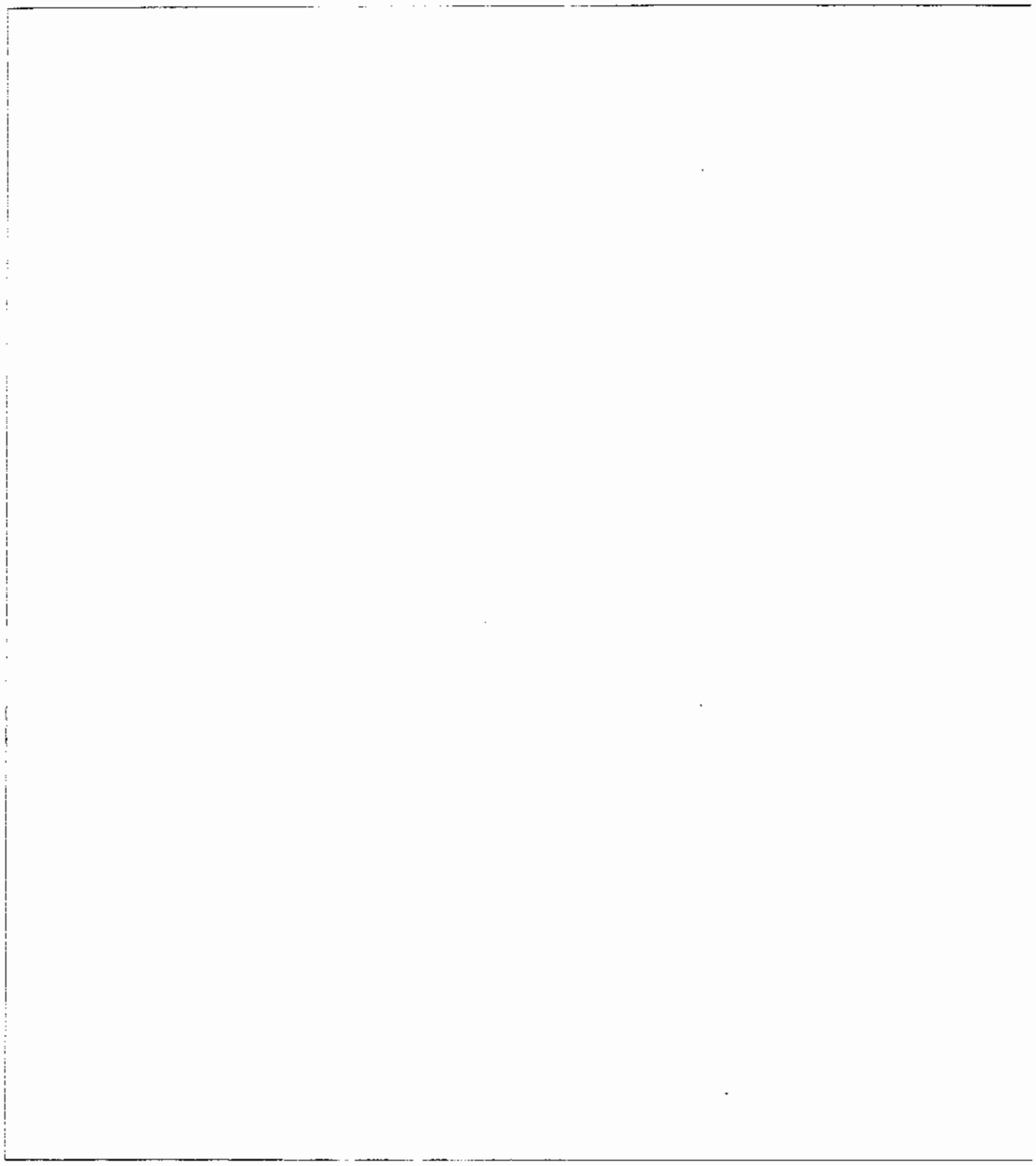

Figure 6: D0 Test Beam muon energy distribution (in ADC counts) seen in a calorimeter cell at $\eta = 0.05$ in a) CCEM layer 3, b) CCEM layer 4, c) CCEM layer 1, and d) CCEM layer 2.

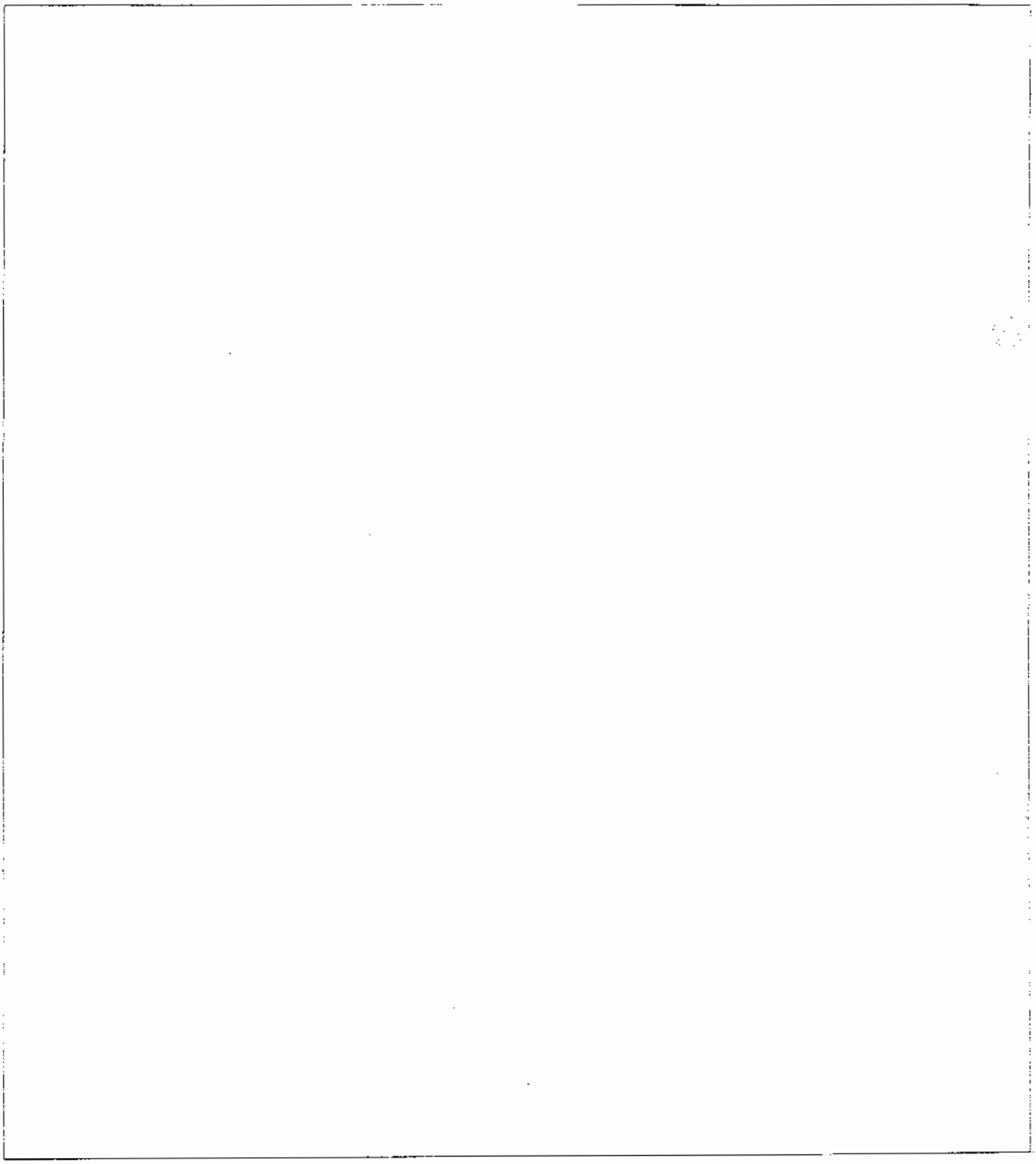

Figure 7: D0 Test Beam muon energy distribution (in ADC counts) seen in a calorimeter cell at $\eta = 0.05$ in a) CCFH layer 3, a) CCCH , a) CCFH layer 1, and a) CCFH layer 2.

Figure 8: D0 Test Beam muon energy distribution (in ADC counts) seen in a calorimeter cell at $\eta = 2.5$ in a) ECEM layer 3, b) ECEM layer 4, c) ECEM layer 1, and d) ECEM layer 2.

Figure 9: D0 Test Beam muon energy distribution (in ADC counts) seen in a calorimeter cell at $\eta = 2.5$ in a) ECIH layer 1-4, and b) ECIH layer 5.

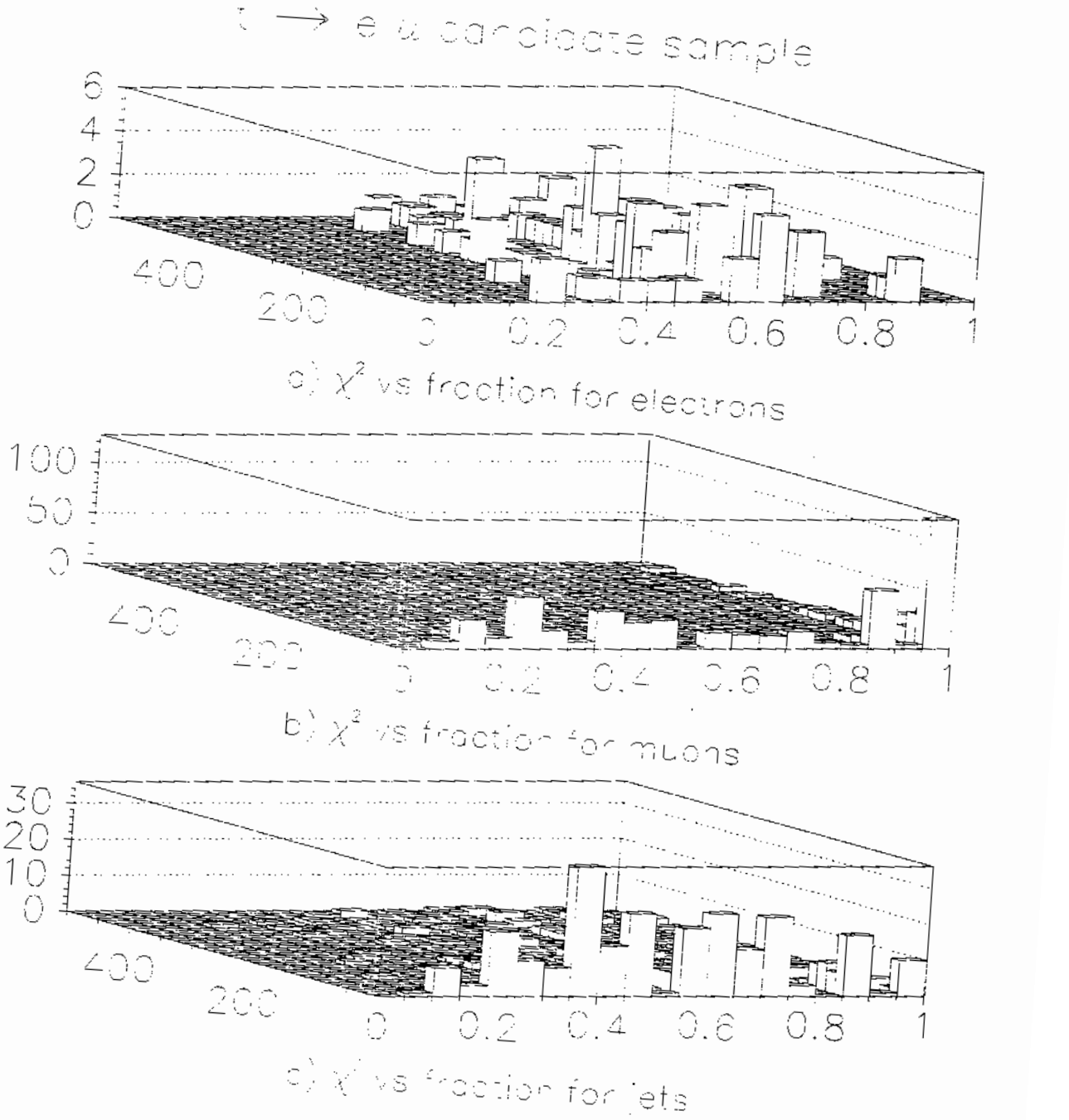

Figure 10: The χ^2 versus the fraction of layers hit for all a) electrons, b) muons and c) jets in the $t \to e\mu$ final candidate sample. Muons are characterized by low χ^2 and a high fraction of layers hit.

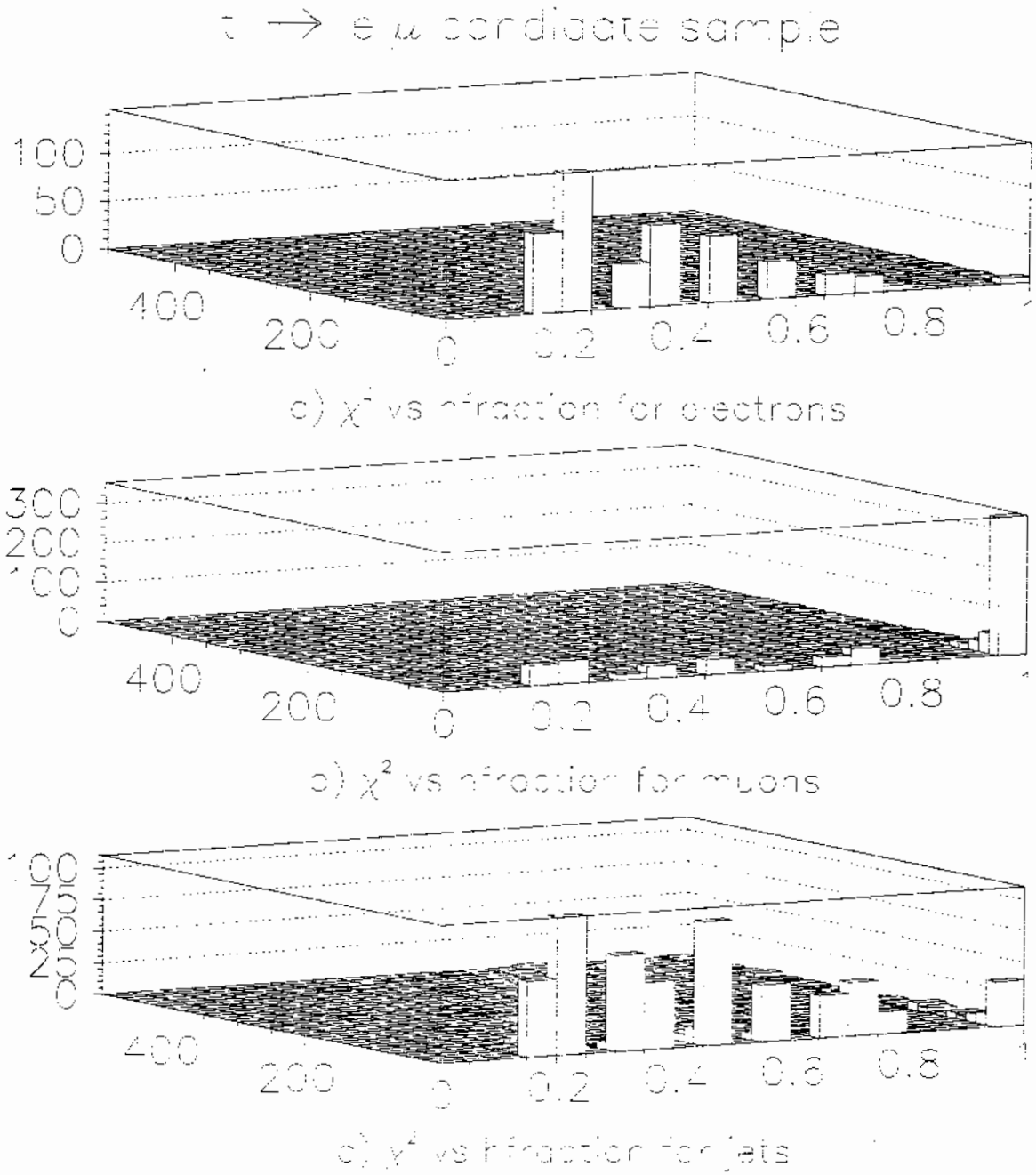

Figure 11: The χ^2 versus the fraction of layers hit in the hadronic calorimeter for all a) electrons, b) muons and c) jets in the $t \rightarrow e\mu$ final candidate sample. Muons are characterized by low χ^2 and a high fraction of layers hit.

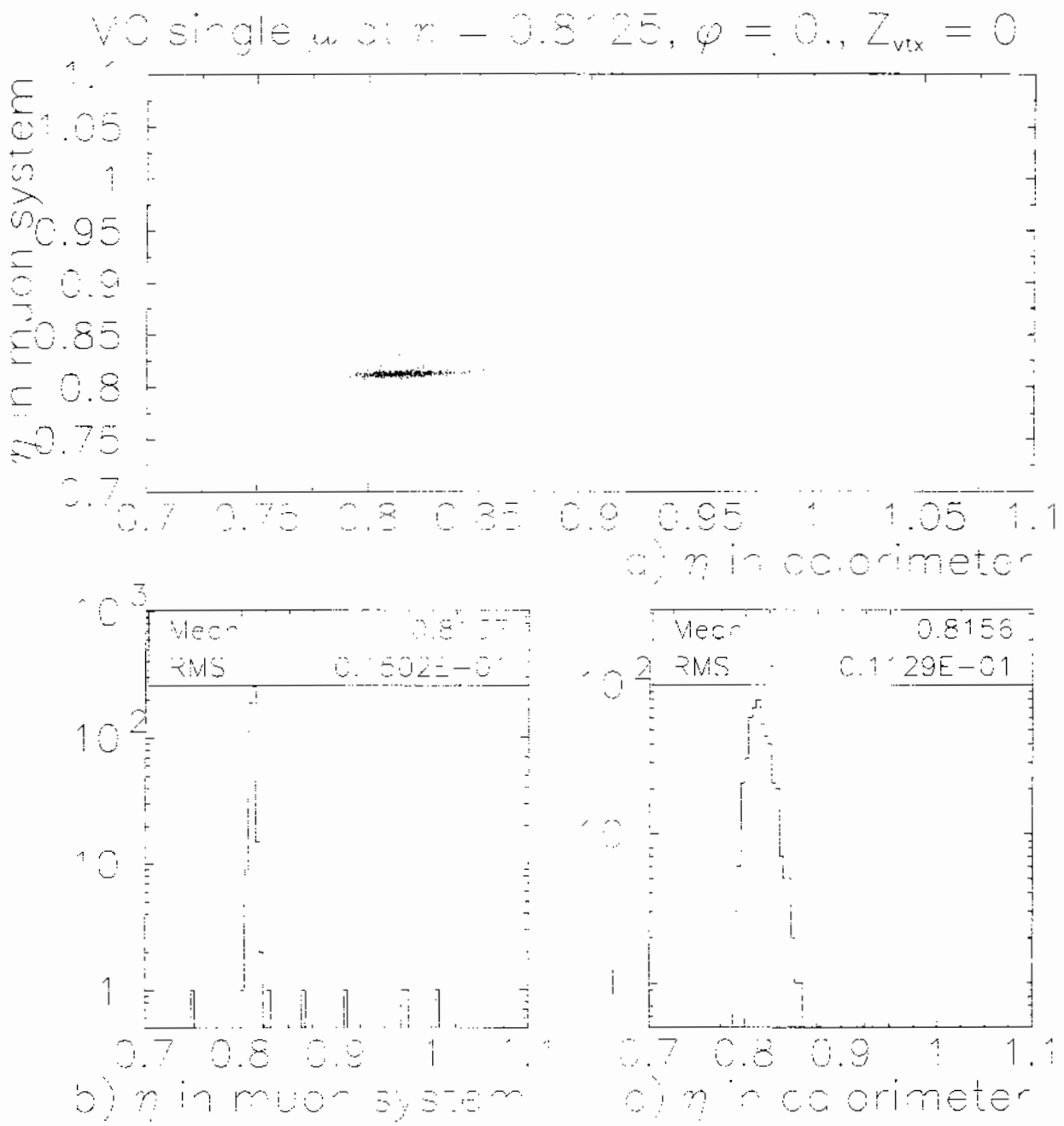

Figure 12: a) Reconstructed η of the muon system versus the reconstructed η of the calorimeter for the 500 MC single muons generated at $\eta = 0.8125, \phi = 0$. To compare muon and calorimeter tracking resolution, plots b) and c) are the projections of the scatterplot in a).

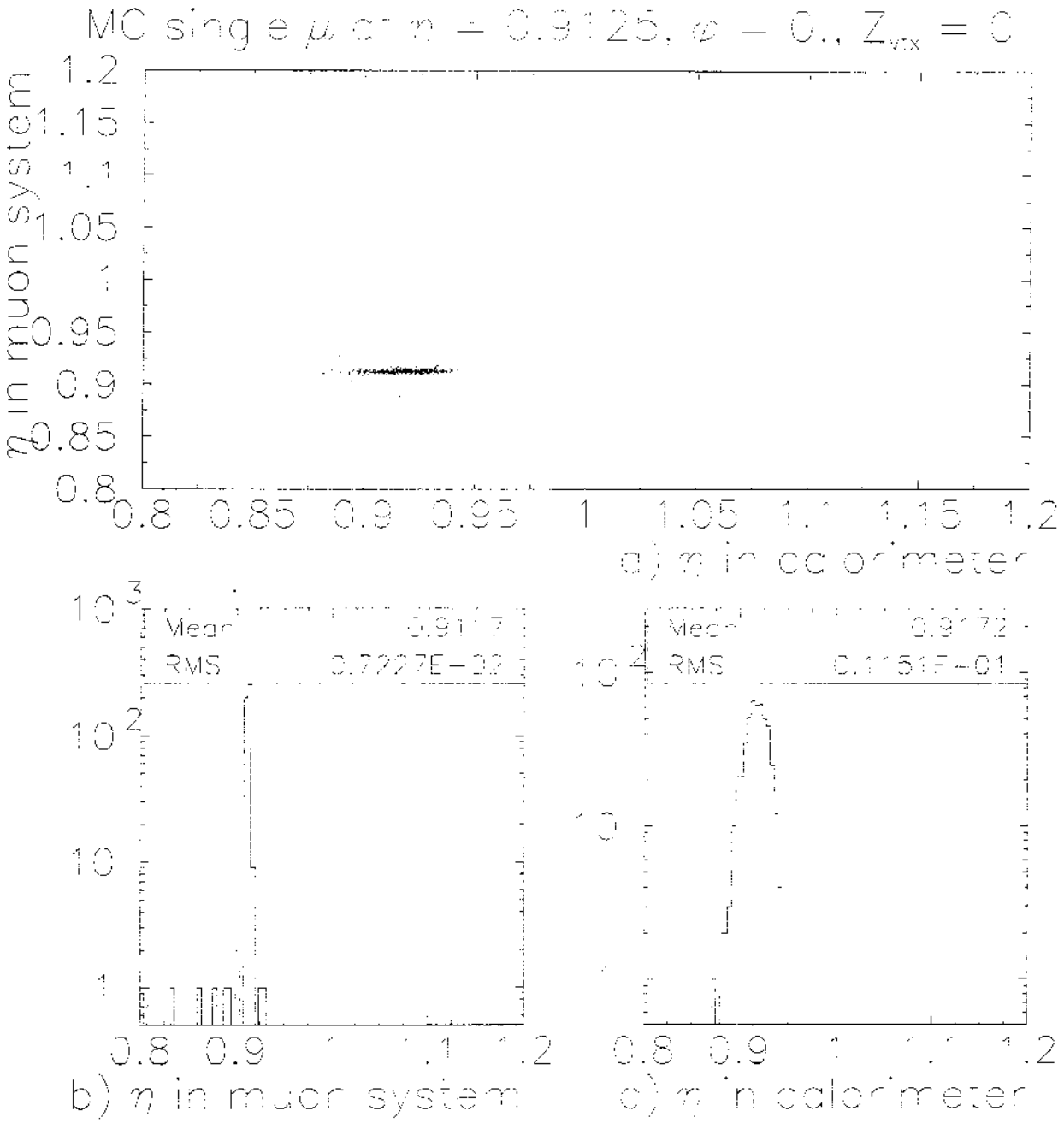

Figure 13: a) Reconstructed η of the muon system versus the reconstructed η of the calorimeter for the 500 MC single muons generated at $\eta = 0.9125, \phi = 0$. To compare muon and calorimeter tracking resolution, plots b) and c) are the projections of the scatterplot in a).

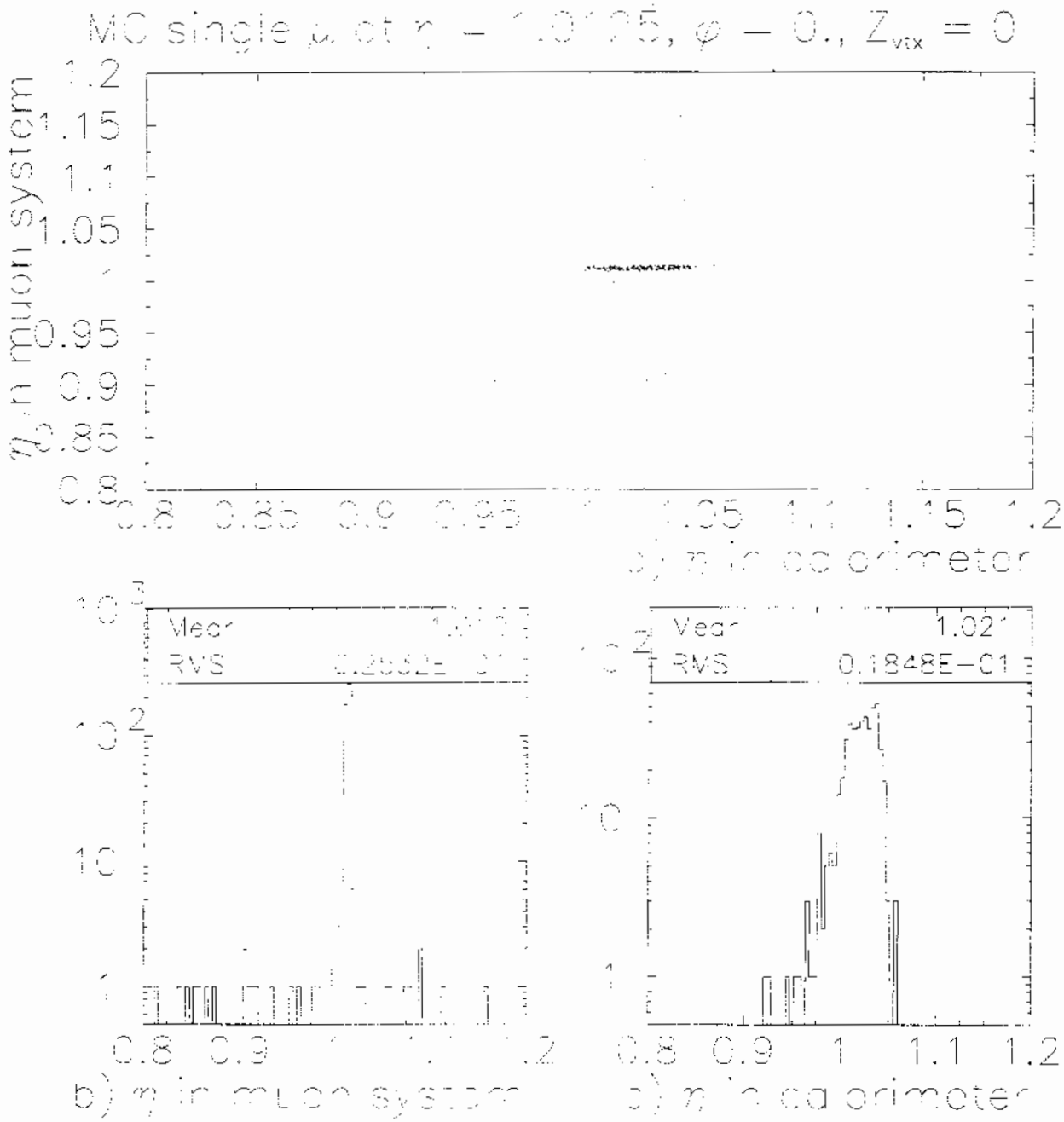

Figure 14: a) Reconstructed η of the muon system versus the reconstructed η of the calorimeter for the 500 MC single muons generated at $\eta = 1.0125, \phi = 0$. To compare muon and calorimeter tracking resolution, plots b) and c) are the projections of the scatterplot in a).

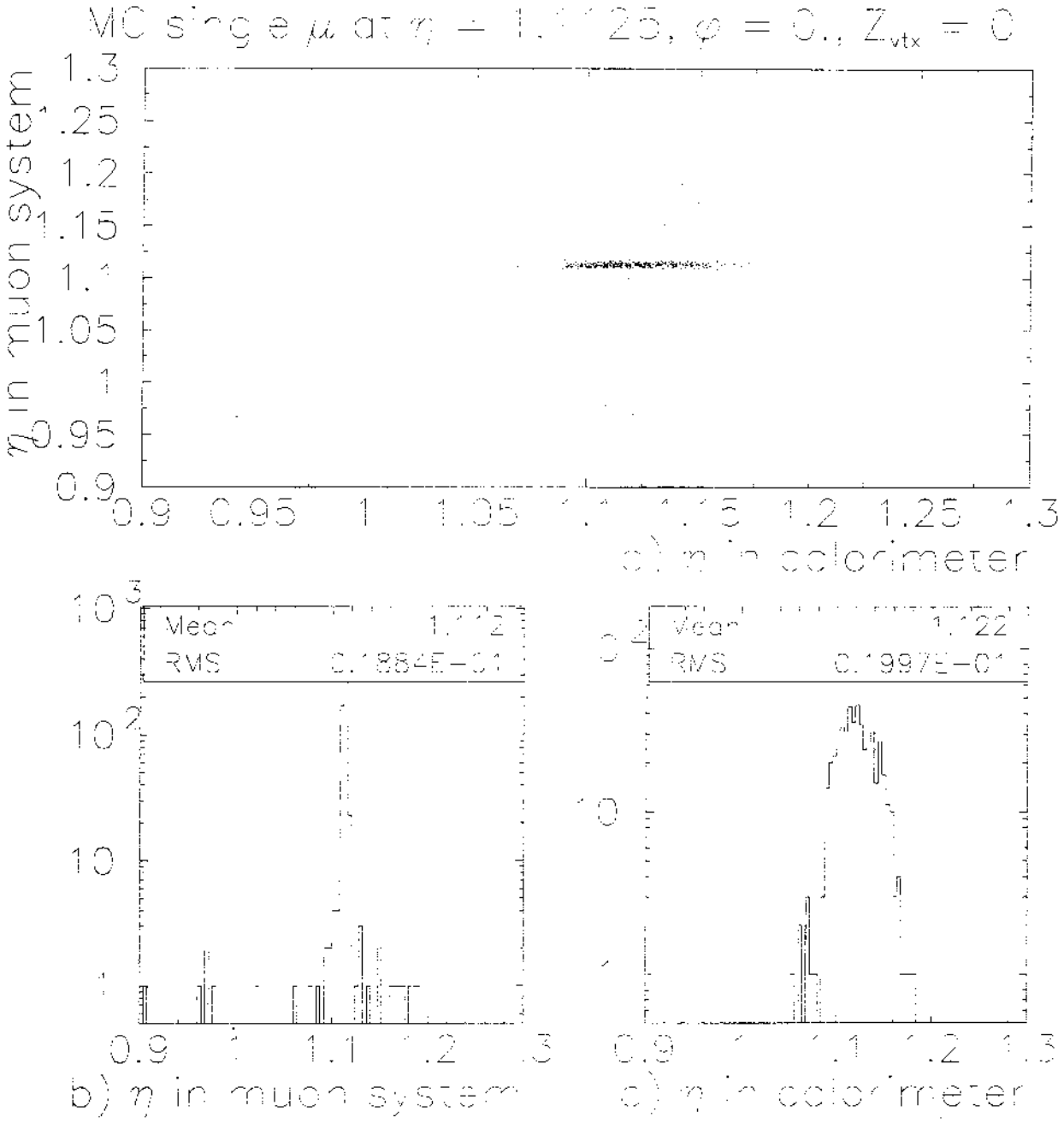

Figure 15: a) Reconstructed η of the muon system versus the reconstructed η of the calorimeter for the 500 MC single muons generated at $\eta = 1.1125, \phi = 0$. To compare muon and calorimeter tracking resolution, plots b) and c) are the projections of the scatterplot in a).

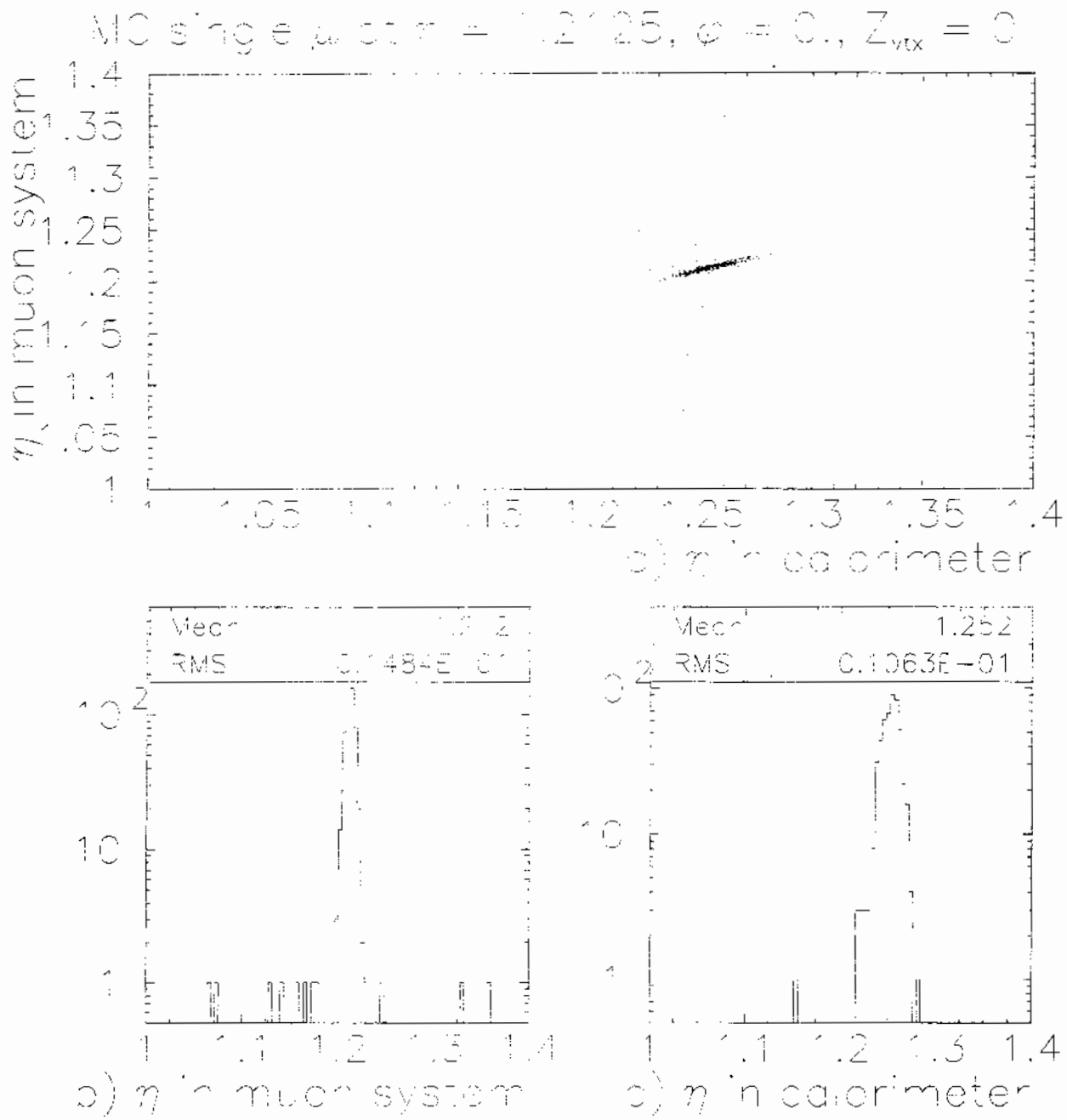

Figure 16: a) Reconstructed η of the muon system versus the reconstructed η of the calorimeter for the 500 MC single muons generated at $\eta = 1.2125, \phi = 0$. To compare muon and calorimeter tracking resolution, plots b) and c) are the projections of the scatterplot in a).

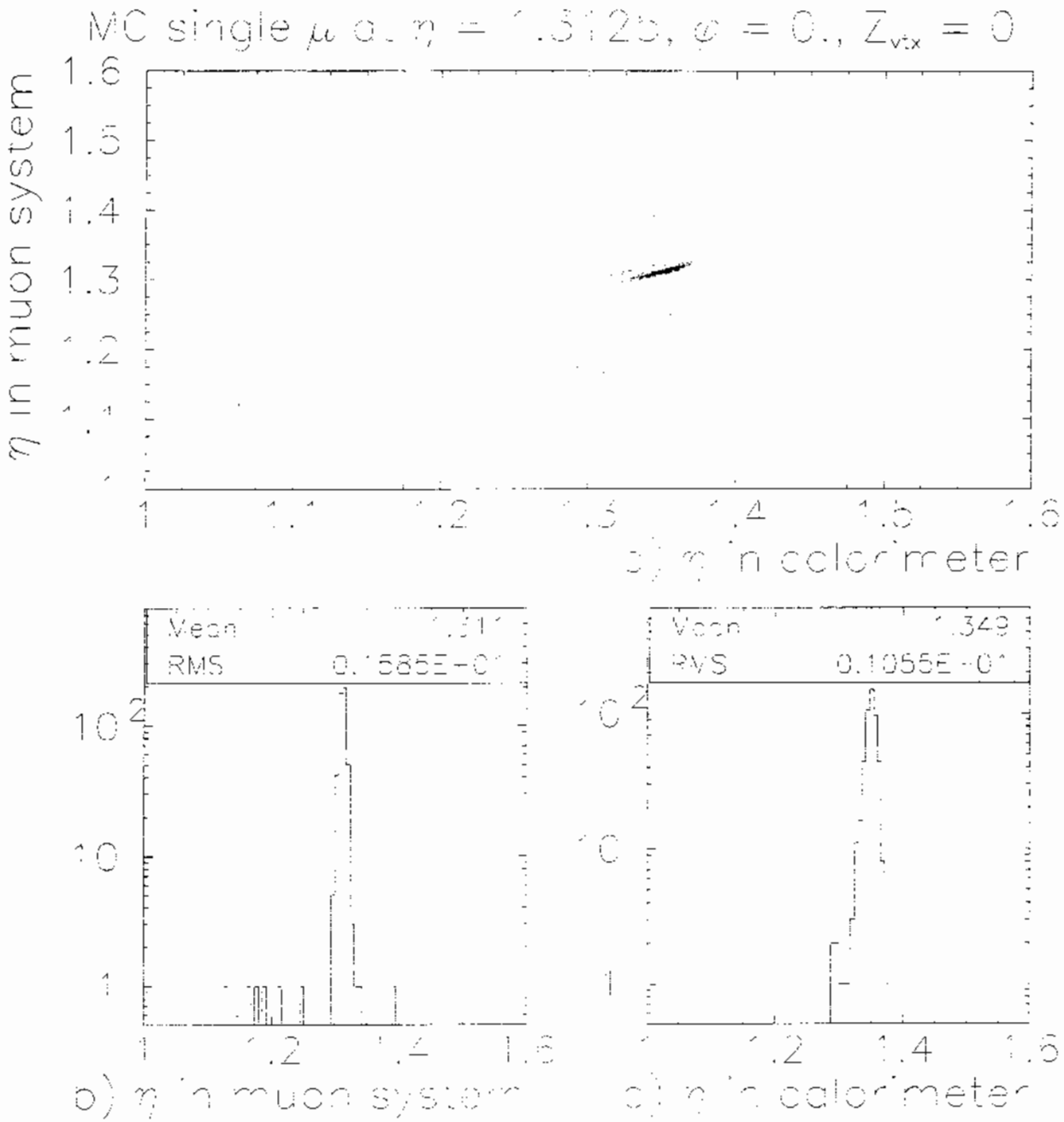

Figure 17: a) Reconstructed η of the muon system versus the reconstructed η of the calorimeter for the 500 MC single muons generated at $\eta = 1.3125, \phi = 0$. To compare muon and calorimeter tracking resolution, plots b) and c) are the projections of the scatterplot in a).

Figure 18: For MC single muons distributed uniformly in η and ϕ space, plot a) shows the reconstructed η of the muon system versus the reconstructed η of the calorimeter. b) is the corresponding ϕ plot.

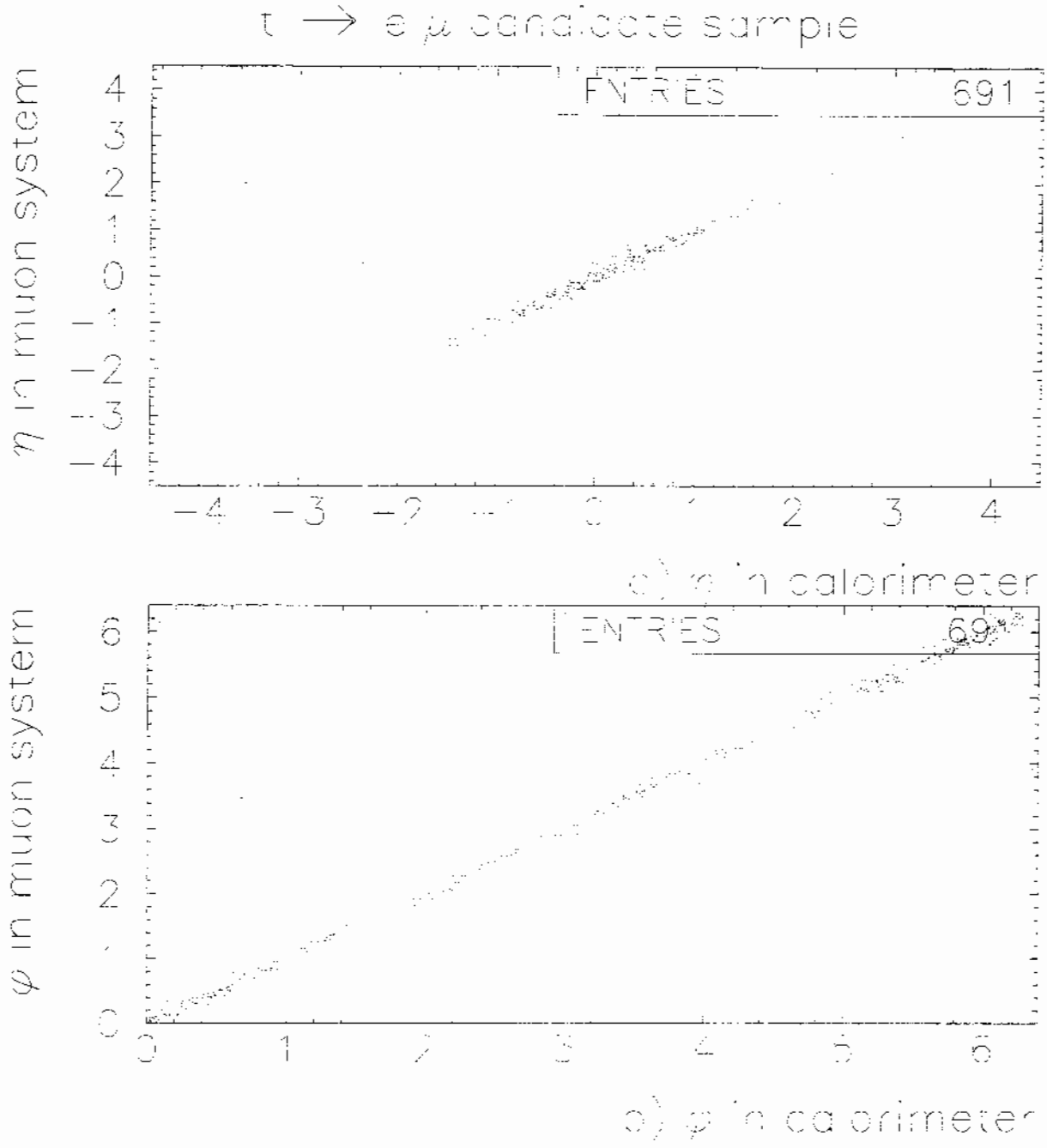

Figure 19: For the $t \rightarrow e\mu$ final candidate sample, plot a) shows the reconstructed η of the muon system versus the reconstructed η of the calorimeter, b) is the corresponding ϕ plot for verified calorimeter tracks with a hadronic fraction of layers hit greater than 0.65.

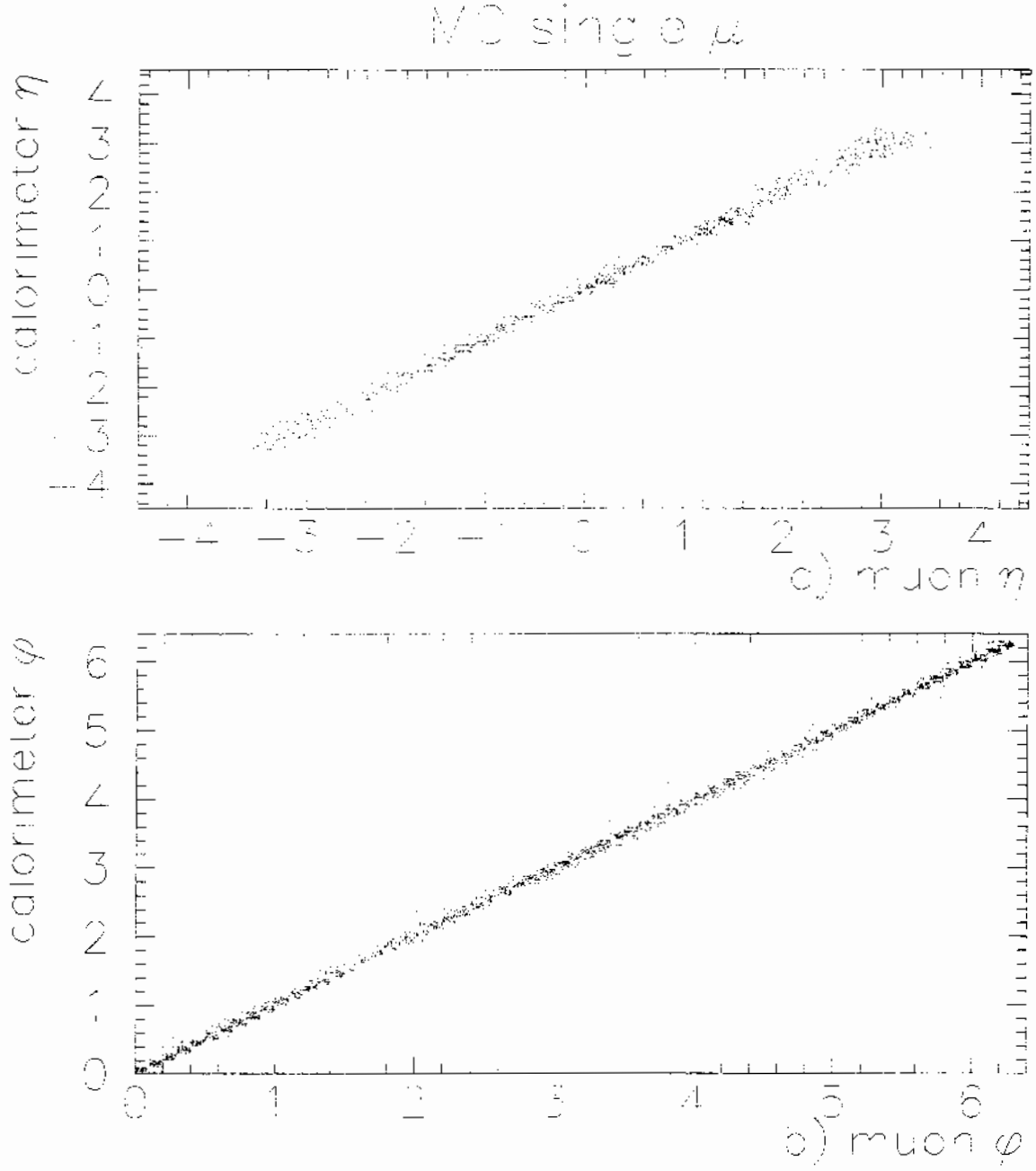

Figure 20: For the reconstructed MC muon sample with muons distributed uniformly in η and ϕ: a) shows the reconstructed η of the calorimeter versus the reconstructed η of the muon system and b) is the corresponding ϕ plot for all 'matched tracks' found. A 'matched track' is a track found in by both the muon system and the MTC μ finding program.

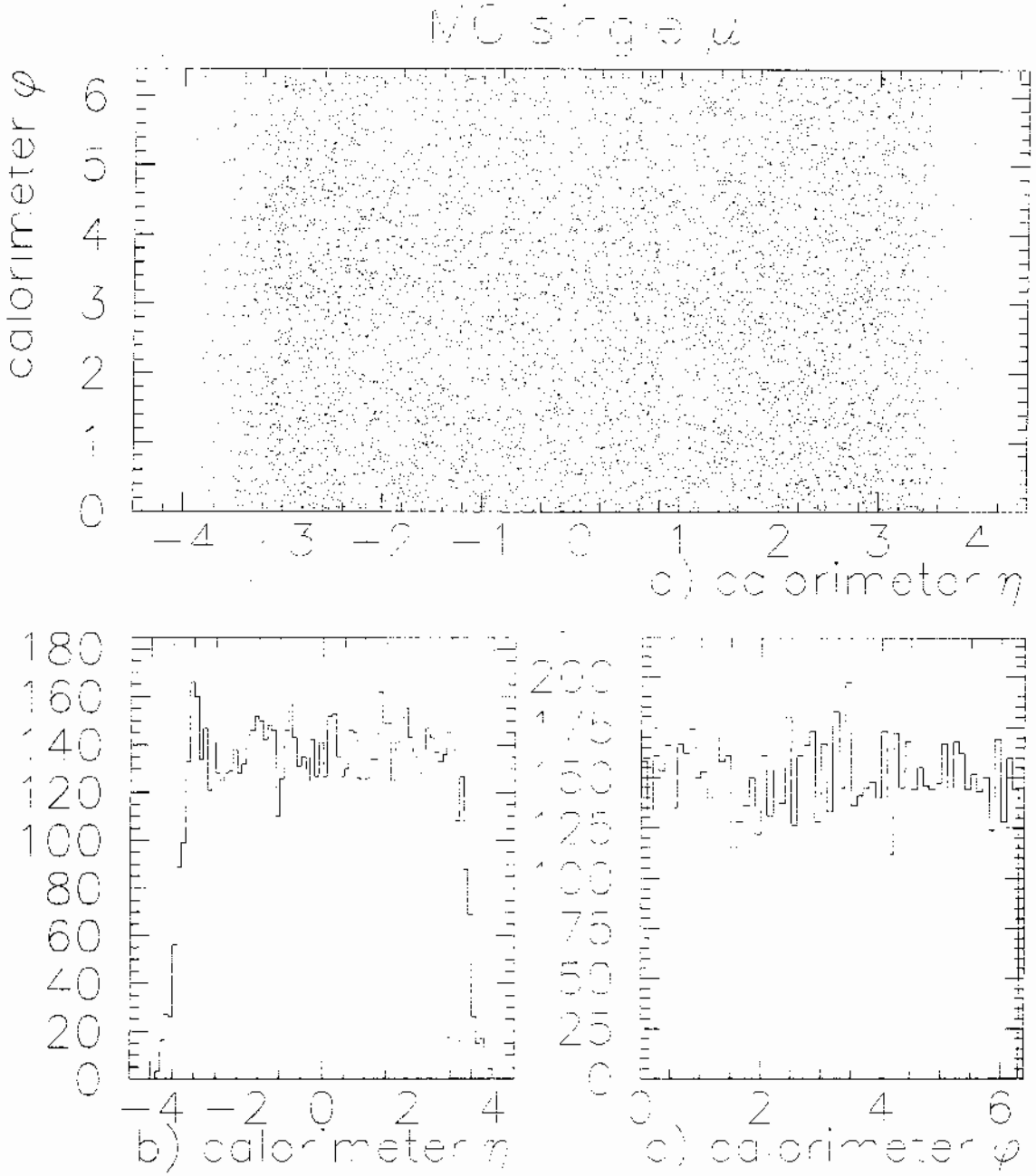

Figure 21: For the reconstructed MC muon sample with muons distributed uniformly in η and ϕ, a) shows the distribution of the MTC found muons in η, ϕ space. b) and c) show the corresponding projections in η and ϕ.

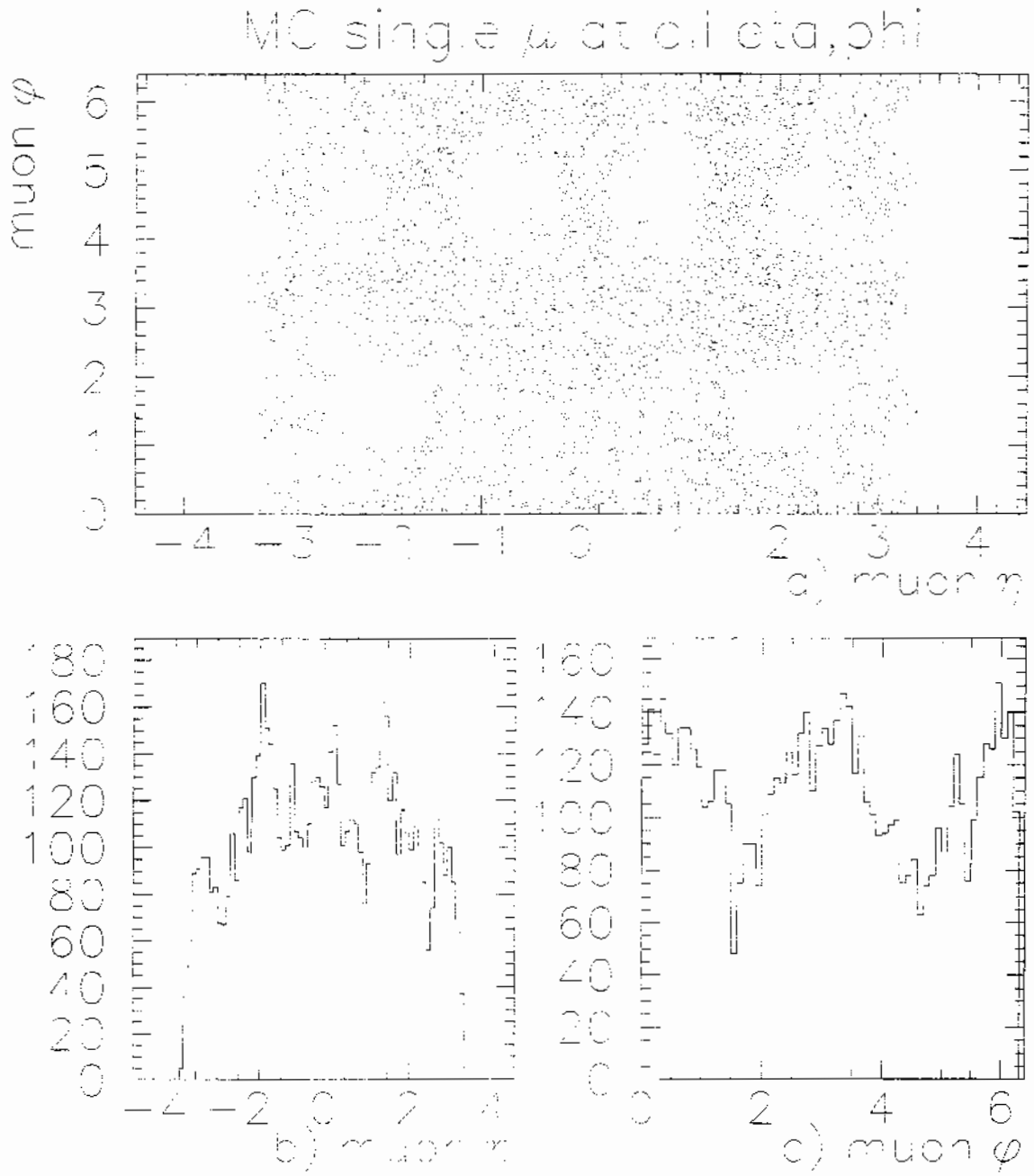

Figure 22: For the reconstructed MC muon sample with muons distributed uniformly in η and ϕ, a) shows the distribution of the muon system (PMUO) found muons in η, ϕ space. b) and c) show the corresponding projections in η and ϕ.

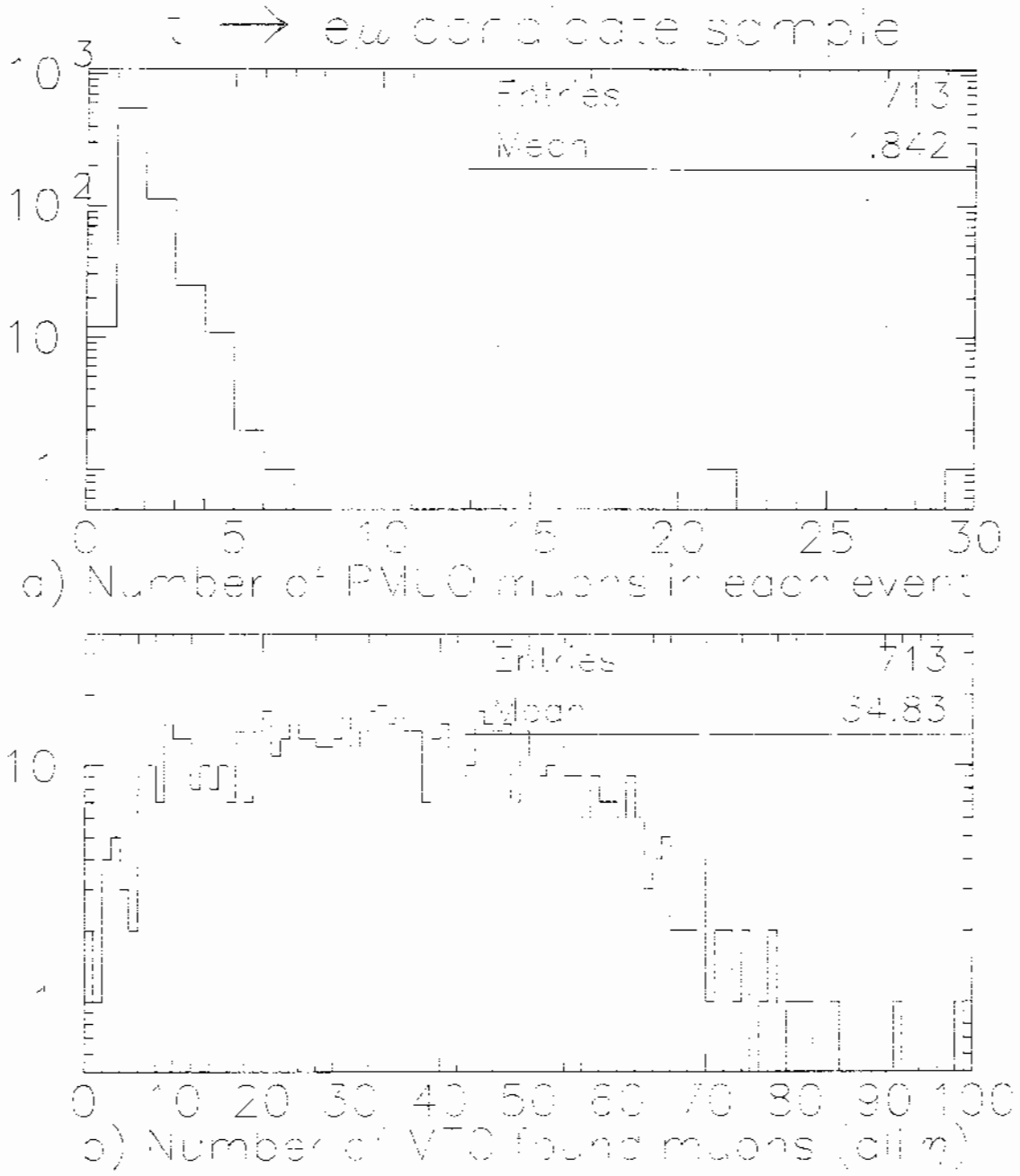

Figure 23: For the muons in the $t \rightarrow e\mu$ final candidate sample, a) and b) shows the number of muons found by the muon system and the MTC μ finding program, respectively.

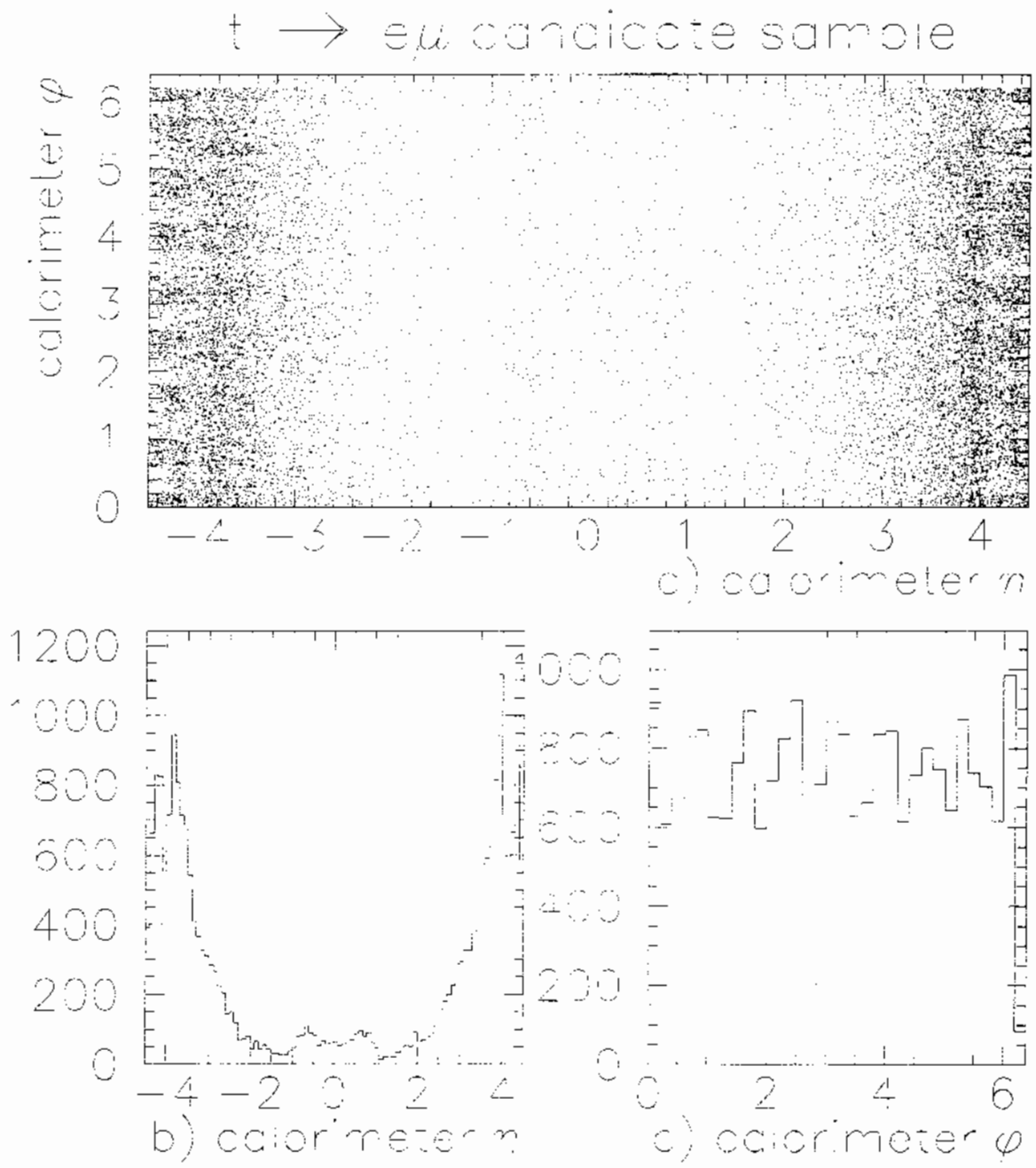

Figure 24: For the $t \rightarrow e\mu$ final candidate sample, a) shows how the MTC found tracks are distributed in η, ϕ space. b) and c) show the corresponding projections in η and ϕ.

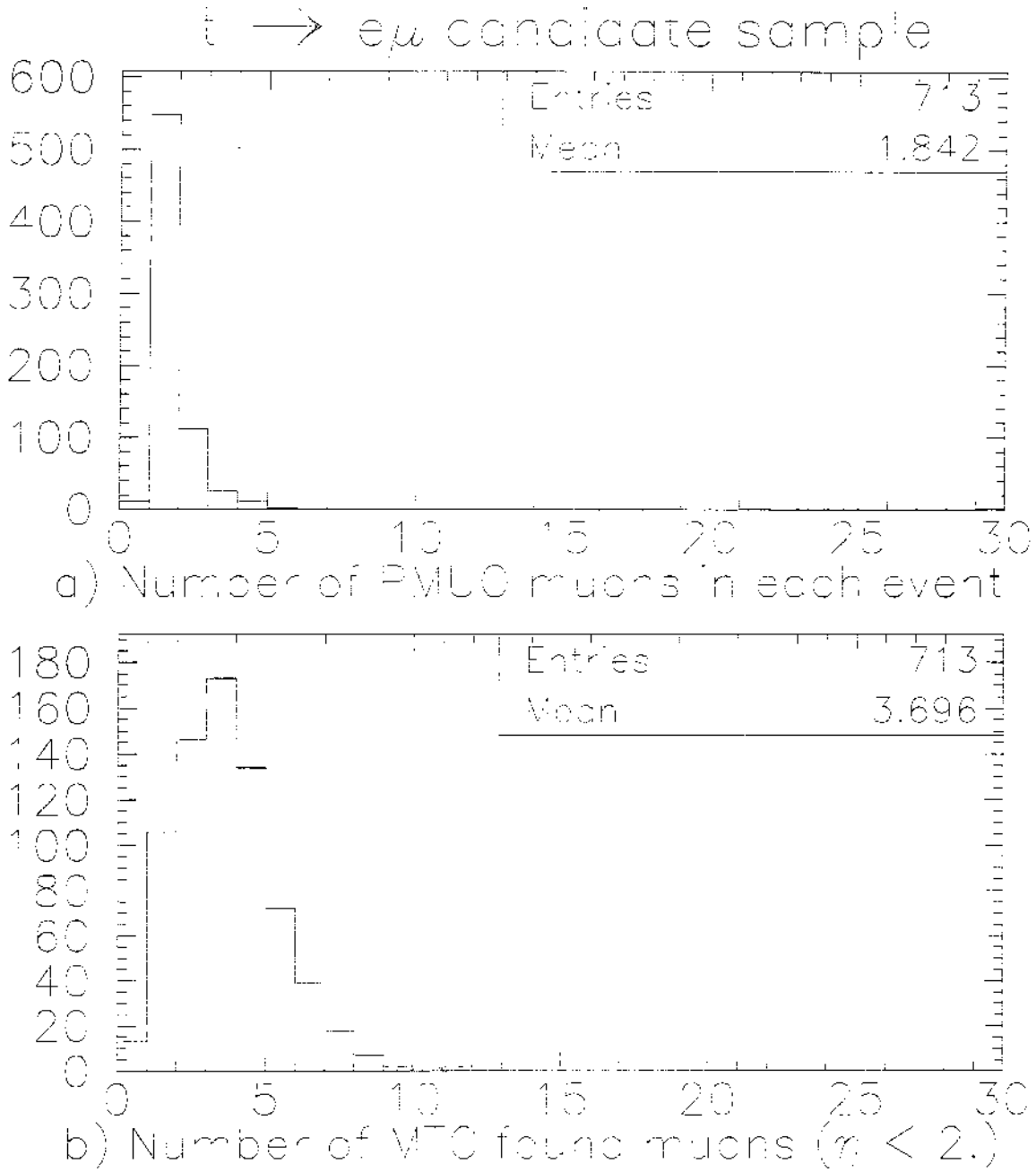

Figure 25: For the muons in the $t \rightarrow e\mu$ final candidate sample, a) shows the number of muons found by the muon system and b) shows the number of muons found by the MTC μ finding program in the η range from -2.0 to 2.0.